

國立臺灣大學工學院化學工程學系



碩士論文

Department of Chemical Engineering

College of Engineering

National Taiwan University

Master's Thesis

多孔球形粒子之暫態緩慢移動
Transient slow motion of a porous sphere

余展維

Chan-Wei Yu

指導教授：葛煥彰 教授

Advisor: Huan-Jang Keh, Professor

中華民國 一百一十三年 七月

July, 2024



國立臺灣大學碩士學位論文
口試委員會審定書

多孔球形粒子之暫態緩慢移動
Transient slow motion of a porous sphere

本論文係余展維君 (R11524095) 在國立臺灣大學化學工程學系所完成之碩士學位論文，於民國一百一十三年七月五日承下列考試委員審查通過及口試及格，特此證明

口試委員：

葛煥利

(簽名)

謝子登

(指導教授)

詹正雄

系主任、所長

廖英志

(簽名)

謝辭



本論文之完成，首先衷心感謝我的指導教授 葛煥彰老師。感謝老師於我研究期間的悉心指導，在研究遭遇困難時協助我釐清問題，並以其淵博的專業知識提供我研究建議，使我得以解決問題並順利完成論文。同時也感謝老師給我擔任流體力學及操作與高等流體力學助教的機會，不只讓我對流體力學有更加深入的理解從而找出論文問題的解決方向，也使我累積許多課堂之外的經驗，獲益良多，在此向老師獻上由衷的感謝。此外，承蒙口試委員詹正雄教授以及謝子賢博士撥冗校閱審核並提供諸項建議，使本論文得以更佳完備，謹致以最深的謝意。

再來要感謝實驗室的學長、同學及學弟。感謝浚棋學長指導我熟悉研究背景及所需程式，願意抽空與我討論研究相關問題並提供筆記供我參考，也謝謝仁宏和晉宇兩位學長在我剛進入實驗室期間給予各方面的幫助；感謝旻叡推薦我進入這個實驗室，和你討論課業研究或分享趣事使我的研究室生活過得充實且充滿歡樂，很高興能遇到你這樣的朋友；感謝同學家霖和永捷兩年間時常與我相互討論課業或研究上的問題，並且在實驗室事務上提供我各方面的幫助，使我的研究過程更加順利；感謝奕銓、威銓和郁富三位學弟一年以來的熱切協助，你們所提出的問題與意見為我帶來不少啟發，祝學弟們都能順利完成學業。

最後感謝家人於我首次研究所考試失利後的鼓勵與支持，使我能夠走出挫折、全心全意地準備重考，是父母的付出及辛勞才讓我能毫無後顧之憂地完成學業。

謹以此論文，獻給我的家人以及所有幫助過我的朋友們。

余展維 謹識

民國 一百一十三年 七月

摘要

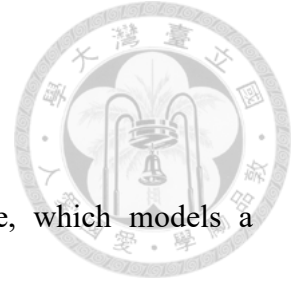


本論文以多孔球形粒子模型模擬可滲透聚合物鏈團或絮聚體等微奈米粒子於不可壓縮牛頓流體中受一恆定力作用所造成之起始緩慢移動。由修正的暫態 Stokes 及 Brinkman 方程式描述多孔球形粒子內外流體之運動狀態並以拉普拉斯轉換分別求解多孔粒子內外的流速分佈，再分析粒子所受拖曳力即可求得轉換 (s) 域中相關變數及粒子暫態速度解析解函數，最後以拉普拉斯逆轉換數值解比較時間 (t) 域中多孔粒子暫態速度和加速度與粒子孔隙度、粒子內流體滲透參數、粒子與流體相對密度和無因次時間等參數間的關係及變化趨勢。

結果顯示，粒子速度如同預期會隨外加力作用時間逐漸增加，並且質量密度較大粒子的速度增長會落後於密度較低的粒子。於大部分條件下，粒子暫態速度會隨粒子孔隙度增加遞增，而高流體滲透性的多孔粒子相較於低滲透性的相同粒子會具有更大的暫態速度，但相對終端速度之速度百分比增長則可能落後於滲透性較小的粒子。多孔粒子的加速度為時間的單調遞減函數及流體滲透性的單調遞增函數。實際應用上，多孔粒子的暫態蠕動行為可能比不可滲透粒子更加重要。

關鍵詞：起始移動，多孔粒子，暫態速度，粒子蠕動，拖曳力

Abstract



The start-up creeping motion of a porous spherical particle, which models a permeable polymer coil or floc of nanoparticles, in an incompressible Newtonian fluid generated by the sudden application of a body force is investigated for the first time. The transient Stokes and Brinkman equations governing the fluid velocities outside and inside the porous sphere, respectively, are solved by using the Laplace transform. An analytical formula for the transient velocity of the particle as a function of relevant parameters is obtained.

As expected, the particle velocity increases over time, and a particle with greater mass density lags behind a corresponding less dense particle in the growth of the particle velocity. In general, the transient velocity is an increasing function of the porosity of the particle. On the other hand, a porous particle with a higher fluid permeability will have a greater transient velocity than the same particle with a lower permeability, but may trail behind the less permeable particle in the percentage growth of the velocity. The acceleration of the porous particle is a monotonic decreasing function of the elapsed time and a monotonic increasing function of its fluid permeability. In particular, the transient behavior of creeping motions of porous particles may be much more important than that of impermeable particles.



Keywords: start-up migration, porous particle, transient velocity, creeping motion,
hydrodynamic drag force

Table of Contents



論文口試委員審定書	i
謝辭	ii
摘要	iii
Abstract	iv
Table of Contents.....	vi
List of Figures	viii
Chapter 1 Introduction.....	1
Chapter 2 Analysis	4
2.1 Fluid Velocity Field	5
2.2 Transient Migration Velocity.....	10
Chapter 3 Results and Discussion.....	12
3.1 Scaled Particle Mobility.....	12
3.2 Dimensionless Particle Acceleration.....	22
Chapter 4 Conclusions	28
List of Symbols.....	29
References.....	31

Appendix A Start-up Rotation of a Porous Sphere in a Cavity	34
A.1 Introduction	34
A.2 Analysis.....	37
A.3 Results and Discussion.....	43
A.4 Conclusions	62
A.5 References	64





List of Figures

Figure 1. Geometric sketch for the transient motion of a porous sphere under an applied force.	4
Figure 2a. The scaled particle mobility $6\pi\eta aU / F_A$ versus the dimensionless elapsed time vt/a^2 with $\lambda a = 1$ and $\varepsilon = 0.5$	13
Figure 2b. The scaled particle mobility $6\pi\eta aU / F_A$ versus the dimensionless elapsed time vt/a^2 with $\rho_p / \rho = 1$ and $\varepsilon = 0.5$	14
Figure 2c. The scaled particle mobility $6\pi\eta aU / F_A$ versus the dimensionless elapsed time vt/a^2 with $\lambda a = 1$ and $\rho_p / \rho = 1$	15
Figure 3a. The scaled particle mobility $6\pi\eta aU / F_A$ at $vt/a^2 = 1$ versus the density ratio ρ_p / ρ with $\varepsilon = 0.5$	16
Figure 3b. The scaled particle mobility $6\pi\eta aU / F_A$ at $vt/a^2 = 1$ versus the density ratio ρ_p / ρ with $\lambda a = 1$	17
Figure 4a. The scaled particle mobility $6\pi\eta aU / F_A$ at $vt/a^2 = 1$ versus the shielding parameter λa with $\varepsilon = 0.5$	18
Figure 4b. The scaled particle mobility $6\pi\eta aU / F_A$ at $vt/a^2 = 1$ versus the shielding parameter λa with $\rho_p / \rho = 1$	19

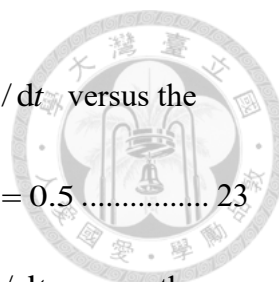


Figure 5a. The dimensionless particle acceleration $(6\pi\rho a^3 / F_A)dU / dt$ versus the dimensionless elapsed time vt / a^2 with $\lambda a = 1$ and $\varepsilon = 0.5$ 23

Figure 5b. The dimensionless particle acceleration $(6\pi\rho a^3 / F_A)dU / dt$ versus the dimensionless elapsed time vt / a^2 with $\rho_p / \rho = 1$ and $\varepsilon = 0.5$ 24

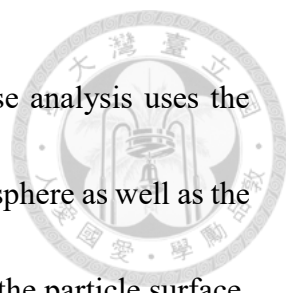
Figure 5c. The dimensionless particle acceleration $(6\pi\rho a^3 / F_A)dU / dt$ versus the dimensionless elapsed time vt / a^2 with $\lambda a = 1$ and $\rho_p / \rho = 1$ 25

Chapter 1 Introduction



The motions of small particles in viscous fluids at vanishingly low Reynolds numbers continue to be of widespread interest to researchers in the areas of chemical, biomedical, mechanical, civil, and environmental engineering. Most of these motions are basic in nature, but enable us to develop reasonable understanding of various practical systems, such as sedimentation, agglomeration, electrophoresis, microfluidics, motion of cells in blood vessels, rheology of suspensions, spray drying, and aerosol technology. Analytical examination of this discipline originates from Stokes' (1851) pioneering work on the creeping motion of slip-free spherical particles in a viscous fluid at steady state and extends to the motion of solid spheres with slip surfaces (Basset 1888) and fluid spheres (Hadamard 1911, Rybczynski 1911).

Being a good model for a polymer coil in a solvent and for a floc of nanoparticles in a colloidal suspension, the problem of a porous particle translating permeably and slowly relative to a viscous fluid has been analyzed rigorously. Sutherland and Tan (1970) used the Stokes equations for the external creeping flow around a settling porous sphere and Darcy's law for the internal flow with the same viscosity as well as the continuity in tangential fluid velocity for the boundary condition at the surface of the particle to obtain a formula relating the particle velocity to the applied force and concluded that it is reasonable for a porous sphere on the assumption of immobilized fluid inside the particle.

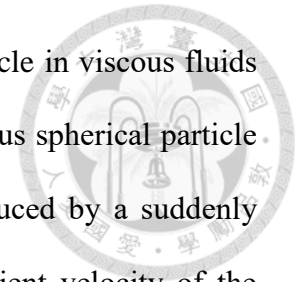


Their conclusion was proven incorrect by Neale *et al* (1973), whose analysis uses the equation of Brinkman (1947) for the creeping flow inside the porous sphere as well as the continuity in fluid velocity and stress for the boundary conditions at the particle surface.

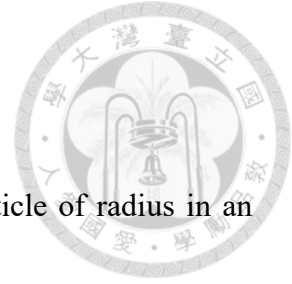
Experimental investigations on settling porous particles at low Reynolds numbers have been performed by Matsumoto and Sukanuma (1977) and Masliyah and Polikar (1980), whose results agree well with the analytical prediction from using the Brinkman equation.

Although the basic formulas for creeping motions of solid, fluid, and porous particles were derived mainly for the steady state, their transient behaviors are also important (Michaelides 1997, Gomez-Solano and Bechinger 2015, Fakour 2018, Buonocore 2019, Li and Keh 2020, 2021). The time evolution of particle velocity is pertinent to applications of various motions in colloidal dynamics with the scale of milliseconds to seconds (Dill and Balasubramaniam 1992, Yossifon *et al* 2009, Sharanya and Raja Sekhar 2015, Premlata and Wei 2020, Lai and Keh 2020, 2021). Many researchers have examined the low Reynolds number response of hydrodynamic forces acting on particles to unsteady translational velocities or unsteady viscous fluid flows (Feng and Joseph 1995, Prakash and Raja Sekhar 2012, Ashmawy 2012, 2017, Prakash and Satyanarayana 2021). On the other hand, the transient responses in the particle velocity to the step change in external force have been analyzed for a no-slip solid sphere (Basset 1888, Keh and Huang 2005), a slip solid sphere (Morrison and Reed 1975), and a fluid sphere (Stewart and Morrison 1981).

As yet, the starting transient creeping motion of a porous particle in viscous fluids has not been studied. In this thesis, the start-up migration of a porous spherical particle with arbitrary mass density, porosity, and fluid permeability produced by a suddenly applied body force is analyzed. An explicit formula for the transient velocity of the particle is obtained in Laplace transform in equation (24).



Chapter 2 Analysis



We consider the transient migration of a porous spherical particle of radius a in an incompressible Newtonian fluid caused by a suddenly applied body force, as illustrated in figure 1. At the initial time, a constant force (such as the gravitational force minus the buoyant force, where \mathbf{e}_z is the unit vector in the direction) is exerted on the initially stationary particle and continues. The spherical coordinate system takes the center of the particle as the origin and \mathbf{e}_z is the axis in the direction. The fluid flow about the spherical particle undergoing rectilinear motion is axially symmetric with trivial dependency.

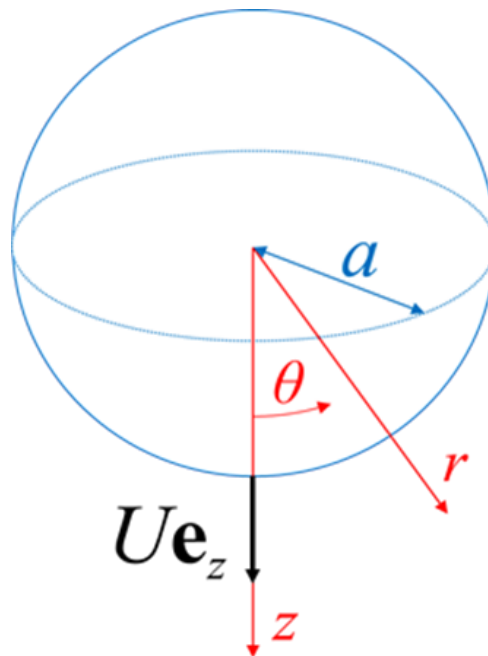
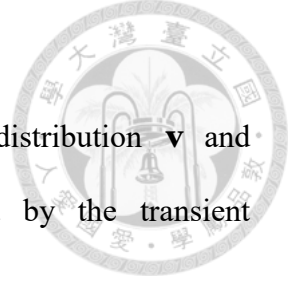


Figure 1. Geometric sketch for the transient motion of a porous sphere under an applied force.



2.1 Fluid Velocity Field

When the Reynolds number is much less than unity, the velocity distribution \mathbf{v} and hydrodynamic pressure profile p of the fluid are governed by the transient Stokes/Brinkman equations in a fixed reference frame:

$$[1-h(r)(1-\varepsilon)]\rho \frac{\partial \mathbf{v}}{\partial t} - \eta \nabla^2 \mathbf{v} + h(r)f(\mathbf{v} - U\mathbf{e}_z) + \nabla p = \mathbf{0}, \quad (1)$$

$$\nabla \cdot \mathbf{v} = 0, \quad (2)$$

where U is the transient migration velocity of the porous sphere (equal to zero at $t = 0$) to be determined, ρ and η are the mass density and viscosity, respectively, of the fluid, ε and f are the porosity and hydrodynamic friction coefficient per unit volume, respectively, of the particle, and $h(r)$ equals 1 and 0 as $r \leq a$ and $r > a$, respectively. In the Brinkman equation [viz., equation (1) for $r \leq a$], \mathbf{v} is the superficial velocity over a volume that is large relative to the pore size but small relative to the particle radius, and the viscosity η is assumed to be the bulk phase value (Neale *et al* 1973). Note that the superficial velocity is an idealized flow velocity calculated as if only the fluid phase present in the porous particle, and thus the fluid density in the Brinkman equation should be modified with the porosity of the particle. The transient Darcy equation, which is the Brinkman equation without the second-order viscous force term, may be applicable for porous particle of low porosity. The transient Darcy equation, which is the Brinkman equation without the second-order viscous force term, may be applicable for porous particle of low porosity.



We employ the stream function Ψ which satisfies equation (2) immediately and relates to the nonvanishing components of the fluid velocity as

$$v_r = -\frac{1}{r^2 \sin \theta} \frac{\partial \Psi}{\partial \theta}, \quad (3a)$$

$$v_\theta = \frac{1}{r \sin \theta} \frac{\partial \Psi}{\partial r}, \quad (3b)$$

Taking the curl of equation (1) and applying equation (3), we obtain

$$E^2 \{ E^2 - h(r) \lambda^2 - [1 - h(r)(1 - \varepsilon)] \frac{1}{\nu} \frac{\partial}{\partial t} \} \Psi = 0, \quad (4)$$

where the axisymmetric Stokes operator E^2 is given by

$$E^2 = \frac{\partial^2}{\partial r^2} + \frac{\sin \theta}{r^2} \frac{\partial}{\partial \theta} \left(\frac{1}{\sin \theta} \frac{\partial}{\partial \theta} \right), \quad (5)$$

$\nu = \eta / \rho$ is the kinematic viscosity of the fluid, and $\lambda = (f / \eta)^{1/2}$ whose reciprocal is the flow penetration length or square root of the fluid permeability in the porous particle.

According to the Blake-Kozeny equation, $1/\lambda$ is proportional to $\varepsilon^{3/2} / (1 - \varepsilon)$ and the pore size (Bird *et al* 2007). For some model porous media made of steel wool and plastic foam slab in organic solutions, experimental values of $1/\lambda$ were found to be about 0.4 mm, while in the surface porous layers of human erythrocytes and grafted polymer microcapsules in salt solutions, values of $1/\lambda$ can be as low as 3 nm (Liu and Keh 1998).

The initial and boundary conditions for the fluid velocity are

$$t = 0: \quad \mathbf{v} = \mathbf{0}, \quad (6)$$

$$r = 0: \quad \mathbf{v} \text{ is finite}, \quad (7)$$

$$r = a: \quad \mathbf{v} \text{ and } \boldsymbol{\tau} - p\mathbf{I} \text{ are continuous}, \quad (8)$$

$$r \rightarrow \infty: \quad \mathbf{v} = \mathbf{0}, \quad (9)$$

where $\boldsymbol{\tau}$ is the viscous stress dyadic of the fluid and \mathbf{I} is the unit dyadic. The steady-state particle velocity is given by (Neale *et al* 1973)

$$U(t \rightarrow \infty) = U_\infty = \frac{F_A}{6\pi\eta a} \left[\frac{\lambda a}{\lambda a - \tanh(\lambda a)} + \frac{3}{2(\lambda a)^2} \right], \quad (10)$$

This terminal velocity, which does not directly depend on the density and porosity of the particle, decreases monotonically with an increase in the shielding parameter λa (ratio of the radius to flow penetration length of the porous particle) from $U_\infty \rightarrow \infty$ for the limiting case $\lambda a = 0$ (fully permeable in the porous particle) to $U_\infty = F_A / 6\pi\eta a$ (the Stokes law) as $\lambda a \rightarrow \infty$ (the particle becomes impermeable). The first term in the brackets of equation (10) becomes unity if Darcy's equation is used to replace Brinkman's equation.

Equations (3)-(9) suggest that the stream function has the form

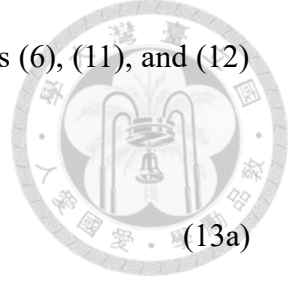
$$\Psi = g(r, t) \sin^2 \theta, \quad (11)$$

Substituting equation (11) into equation (4) and applying the Laplace transform (with a bar over the variable), we obtain

$$\left(\frac{d^2}{dr^2} - \frac{2}{r^2} \right) \left\{ \frac{d^2}{dr^2} - \frac{2}{r^2} - h(r)\lambda^2 - [1 - h(r)(1 - \varepsilon)] \frac{s}{\nu} \right\} \bar{g}(r, s) = 0, \quad (12)$$

where s is the transform parameter.





The general solution for the stream function satisfying equations (6), (11), and (12) is

$$\bar{\Psi} = [C_1 \frac{r^3}{a^3} + C_2 + C_3 \alpha(Br) + C_4 \beta(Br)] \frac{a}{r} \sin^2 \theta \quad \text{if } r \leq a, \quad (13a)$$

$$\bar{\Psi} = [C_5 \frac{r^3}{a^3} + C_6 + C_7 \gamma(Ar) + C_8 \gamma(-Ar)] \frac{a}{r} \sin^2 \theta \quad \text{if } r \geq a, \quad (13b)$$

where

$$\alpha(x) = x \cosh(x) - \sinh(x), \quad (14a)$$

$$\beta(x) = x \sinh(x) - \cosh(x), \quad (14b)$$

$$\gamma(x) = (1-x)e^x, \quad (14c)$$

$$A = \sqrt{s/\nu}, \text{ and } B = \sqrt{\lambda^2 + \varepsilon s/\nu}.$$

The coefficients $C_1, C_2, \dots,$ and C_8 in equation (13) result from the boundary conditions in equations (7)-(9) as

$$C_1 = -a^2 \bar{U} W H, \quad (15a)$$

$$C_3 = 3a^2 \bar{U} W (1 + Aa), \quad (15b)$$

$$C_6 = A^{-2} \bar{U} (2B^2 a^2 W H - \lambda^2 a^2), \quad (15c)$$

$$C_8 = 3A^{-2} \bar{U} W e^{Aa} B^2 a^2 \alpha(Ba), \quad (15d)$$

$$C_2 = C_4 = C_5 = C_7 = 0, \quad (15e)$$

where

$$W = \lambda^2 a^2 [3(1 + Aa)(B^2 - A^2) a^2 \alpha(Ba) + (2B^2 + A^2) a^2 H]^{-1}, \quad (16)$$

$$H = B^2 a^2 [Ba \cosh(Ba) + Aa \sinh(Ba)], \quad (17)$$

Substituting equations (13a) and (15e) into equations (3) and (1), we obtain the Laplace transforms of the internal fluid velocity components and pressure (for $r \leq a$) as

$$\bar{v}_r = -V(r) \cos \theta, \quad (18a)$$

$$\bar{v}_\theta = \frac{1}{2r} \frac{\partial}{\partial r} [r^2 V(r)] \sin \theta, \quad (18b)$$

$$\bar{p} = \frac{\eta r}{a^2} (2B^2 C_1 + \lambda^2 a^2 \bar{U}) \cos \theta, \quad (18c)$$

where

$$V(r) = \frac{2}{a^2} [C_1 + C_3 \alpha (Br) \frac{a^3}{r^3}], \quad (19)$$



2.2 Transient Migration Velocity

The drag force acting on the porous sphere by the fluid in the z direction is negative and given by

$$F_h = 2\pi \int_0^\pi \int_0^a \mathbf{e}_z \cdot f(\mathbf{v} - U\mathbf{e}_z) r^2 \sin\theta dr d\theta, \quad (20)$$

whose magnitude increases monotonically with the elapsed time from naught at $t = 0$ to F_A as $t \rightarrow \infty$. By using equation (1) and the Gauss divergence theorem, equation (20) can also be expressed as

$$F_h = 2\pi a^2 \int_0^\pi [(\tau_{rr} - p) \cos\theta - \tau_{r\theta} \sin\theta]_{r=a} \sin\theta d\theta - 2\pi \varepsilon \rho \int_0^\pi \int_0^a \mathbf{e}_z \cdot \frac{\partial \mathbf{v}}{\partial t} r^2 \sin\theta dr d\theta, \quad (21)$$

where τ_{rr} and $\tau_{r\theta}$ are the normal and shear components, respectively, of the viscous stress $\boldsymbol{\tau}$. Substituting equation (18) into the Laplace transform of equation (20) or (21), we obtain

$$\bar{F}_h = -\frac{4}{3} \pi \eta \lambda^2 a^3 [V(a) + \bar{U}], \quad (22)$$

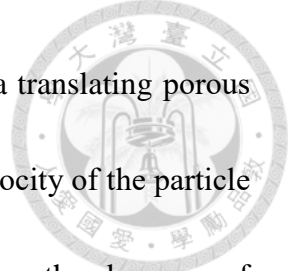
The sum of the applied force and hydrodynamic drag on the particle is equal to the product of its mass and acceleration:

$$F_A + F_h = \frac{4}{3} \pi a^3 (1 - \varepsilon) \rho_p \frac{dU}{dt}, \quad (23)$$

where ρ_p is the mass density of the solid part of the porous particle. The substitution of equation (22) into the Laplace transform of equation (23) results in an explicit formula for the particle migration response to the suddenly applied force,

$$6\pi \eta a \frac{\bar{U}}{F_A} = \frac{9}{2a^2 s} \{ \lambda^2 [1 + 6W(1 + Aa)\alpha(Ba) - 2WH] + A^2 (1 - \varepsilon) \frac{\rho_p}{\rho} \}^{-1}, \quad (24)$$

The transient particle velocity U can be calculated via an inverse Laplace transform of the previous formula numerically (Stehfest 1970, Abate and Valkó 2004).



Note that, if the applied force F_A is suddenly removed from a translating porous sphere already in steady state with the velocity U_∞ , the transient velocity of the particle for the stopping translation will decay from U_∞ to zero following the decrease of $U_\infty - U$ with increasing time given by the inverse transform of equation (24).

In the limit $\lambda a \rightarrow \infty$ (the particle is an impermeable sphere with $\varepsilon = 0$), equation (24) reduces to

$$6\pi\eta a \frac{\bar{U}}{F_A} = \frac{1}{s} \left[1 + Aa + \frac{1}{9} \left(1 + 2 \frac{\rho_p}{\rho} \right) A^2 a^2 \right]^{-1}, \quad (25)$$

and the inverse transform of this formula can be performed analytically (Morrison and Reed 1975, Keh and Huang 2005).

In our linear problem, the transient rotation of the porous sphere caused by an applied torque can be considered separately (see Appendix A).

Chapter 3 Results and Discussion



3.1 Scaled Particle Mobility

In the previous chapter, the starting migration of a porous spherical particle of radius a in an unbounded fluid of viscosity η due to the sudden application of a body force F_A is analyzed. The transient velocity U of the particle calculated from the numerical inverse Laplace transform of equation (24) and scaled by the corresponding steady-state Stokes-law value $F_A / 6\pi\eta a$ is plotted for various values of the scaled elapsed time $\nu t / a^2$, relative density ρ_p / ρ , shielding parameter λa , and porosity ε of the particle in figures 2-4. Similar to the relevant results of an impermeable solid sphere (Morrison and Reed 1975) and fluid sphere (Stewart and Morrison 1981), the scaled migration velocity $6\pi\eta a U / F_A$ of the permeable porous sphere grows continuously with $\nu t / a^2$ from zero at $t = 0$ to the terminal value $6\pi\eta a U_\infty / F_A$ given by equation (10) (which does not depend on ρ_p / ρ or ε) as $t \rightarrow \infty$ for fixed values of ρ_p / ρ , λa , and ε . In the limits of minimum density $\rho_p / \rho = 0$ and maximum porosity $\varepsilon \rightarrow 1$ of the particle, the initial value of $6\pi\eta a U / F_A$ can be obtained by substituting equation (24) into the initial value theorem with the result

$$\lim_{s \rightarrow \infty} (s \cdot \frac{6\pi\eta a}{F_A} \bar{U}) = \lim_{t \rightarrow 0} (\frac{6\pi\eta a}{F_A} U) = \frac{9}{2\lambda^2 a^2}, \quad (26)$$

revealing the singular circumstances at $t = 0$, as shown in figures 2a and 2c.

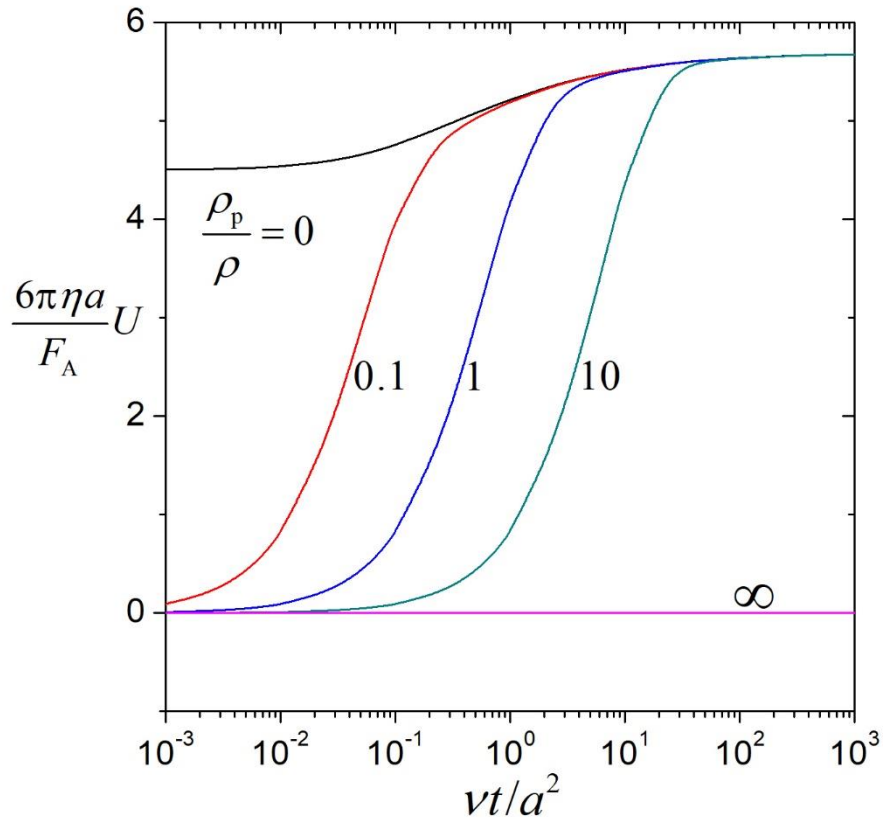


Figure 2a. The scaled particle mobility $6\pi\eta aU / F_A$ versus the dimensionless elapsed time vt/a^2 with $\lambda a = 1$ and $\varepsilon = 0.5$.

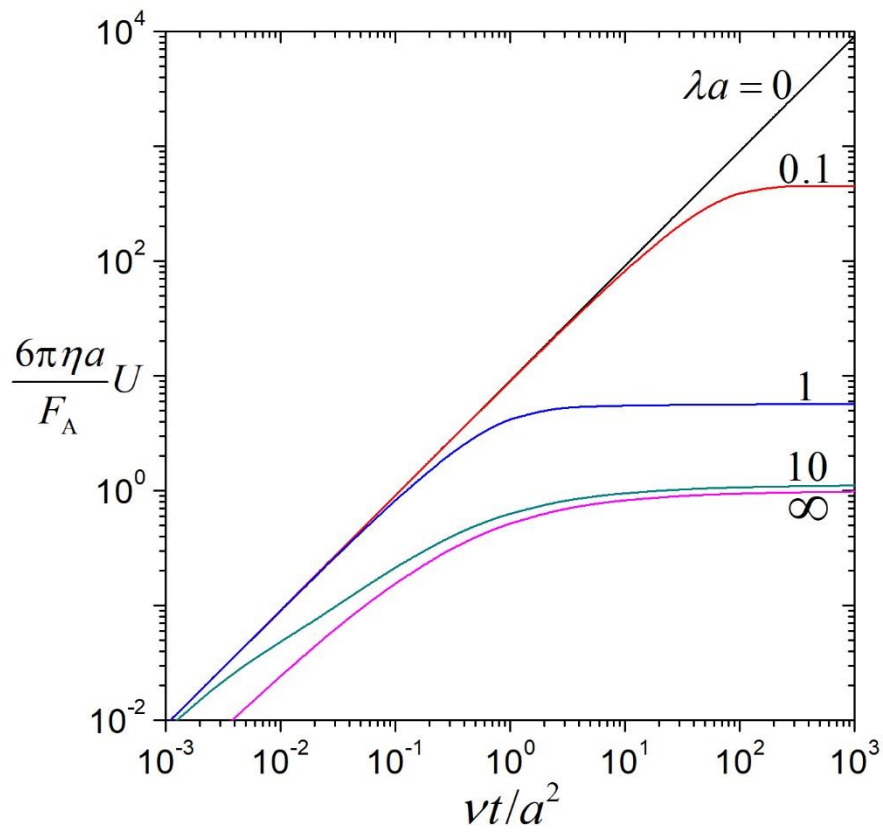


Figure 2b. The scaled particle mobility $\frac{6\pi\eta aU}{F_A}$ versus the dimensionless elapsed time vt/a^2 with $\rho_p/\rho=1$ and $\varepsilon=0.5$.

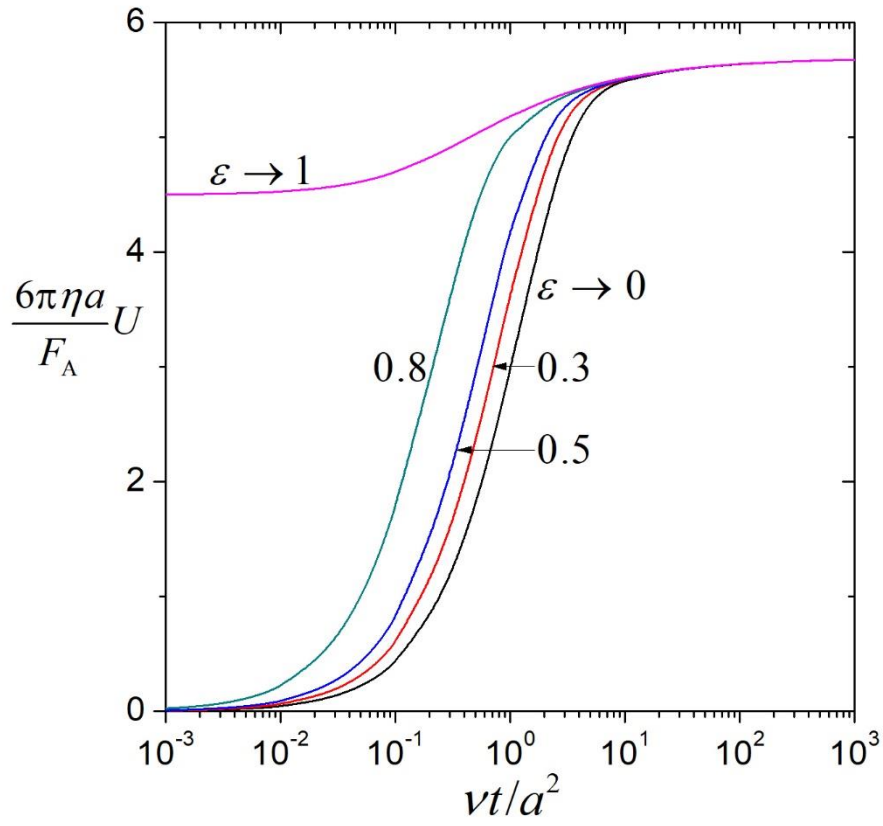


Figure 2c. The scaled particle mobility $\frac{6\pi\eta aU}{F_A}$ versus the dimensionless elapsed time vt/a^2 with $\lambda a=1$ and $\rho_p/\rho=1$.

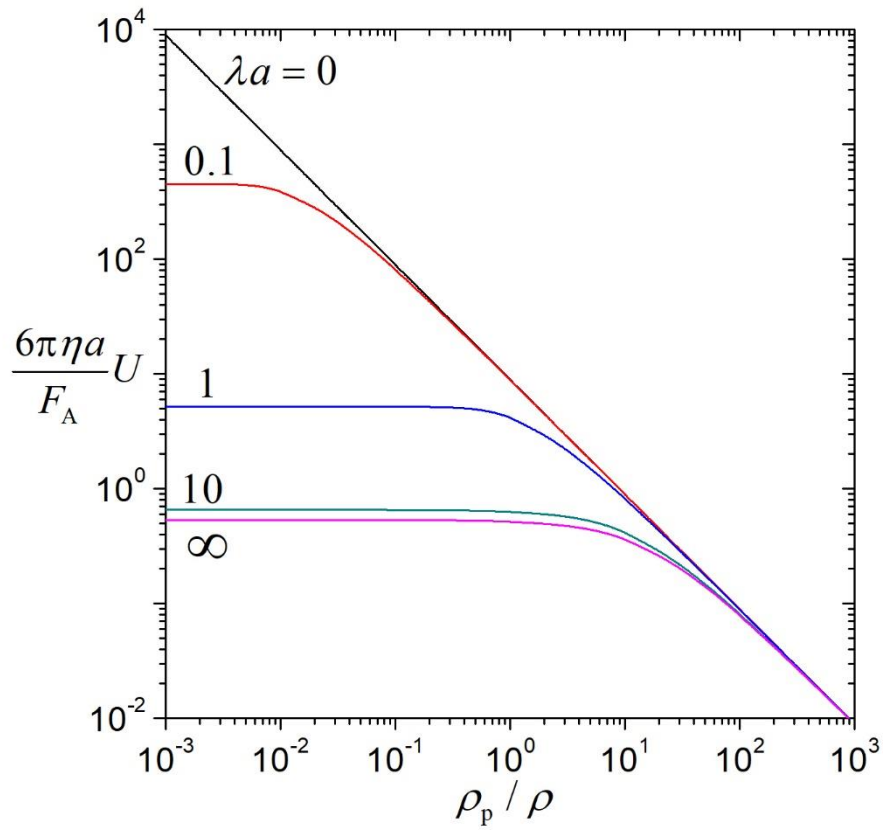


Figure 3a. The scaled particle mobility $\frac{6\pi\eta a U}{F_A}$ at $vt/a^2 = 1$ versus the density ratio ρ_p / ρ with $\varepsilon = 0.5$.

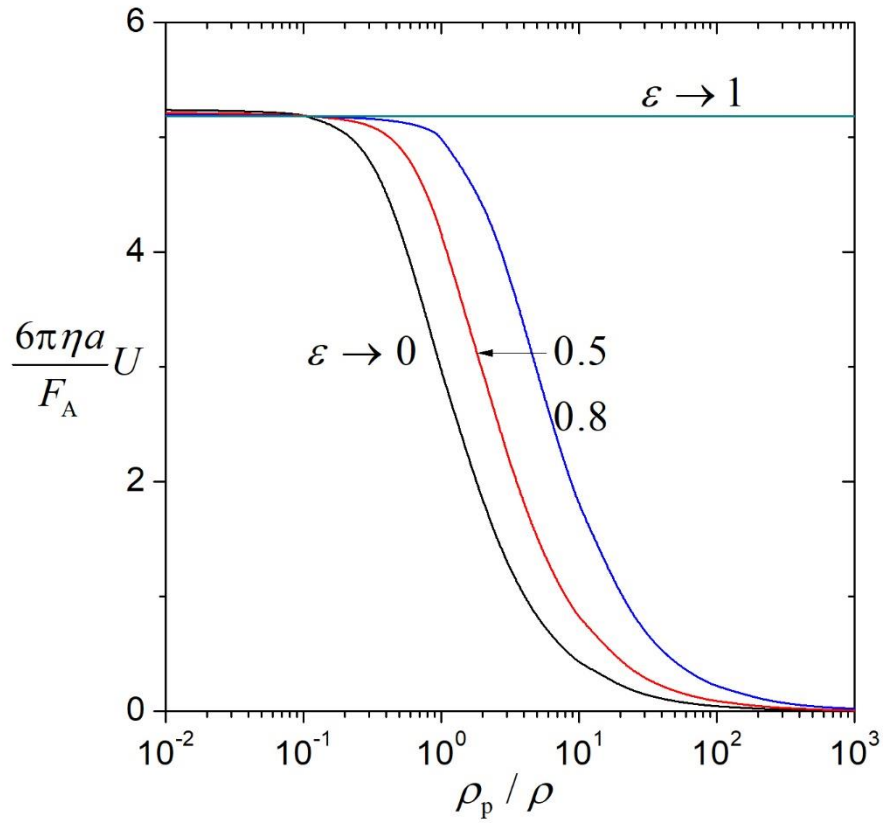


Figure 3b. The scaled particle mobility $6\pi\eta aU/F_A$ at $vt/a^2=1$ versus the density ratio ρ_p/ρ with $\lambda a=1$.

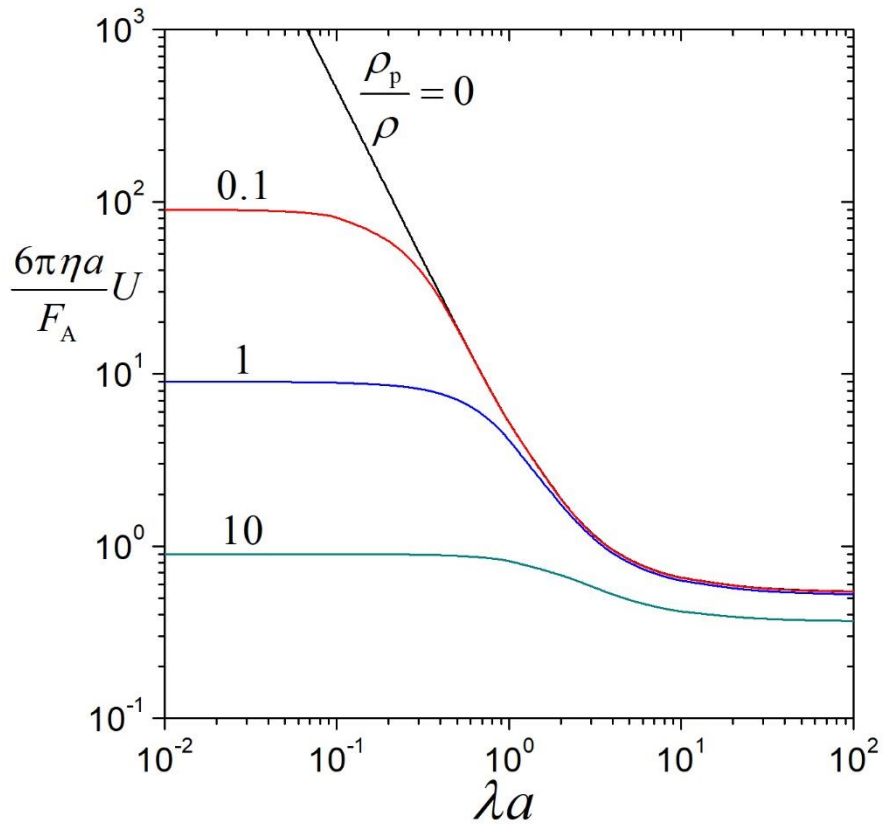


Figure 4a. The scaled particle mobility $\frac{6\pi\eta a U}{F_A}$ at $vt/a^2 = 1$ versus the shielding parameter λa with $\varepsilon = 0.5$.

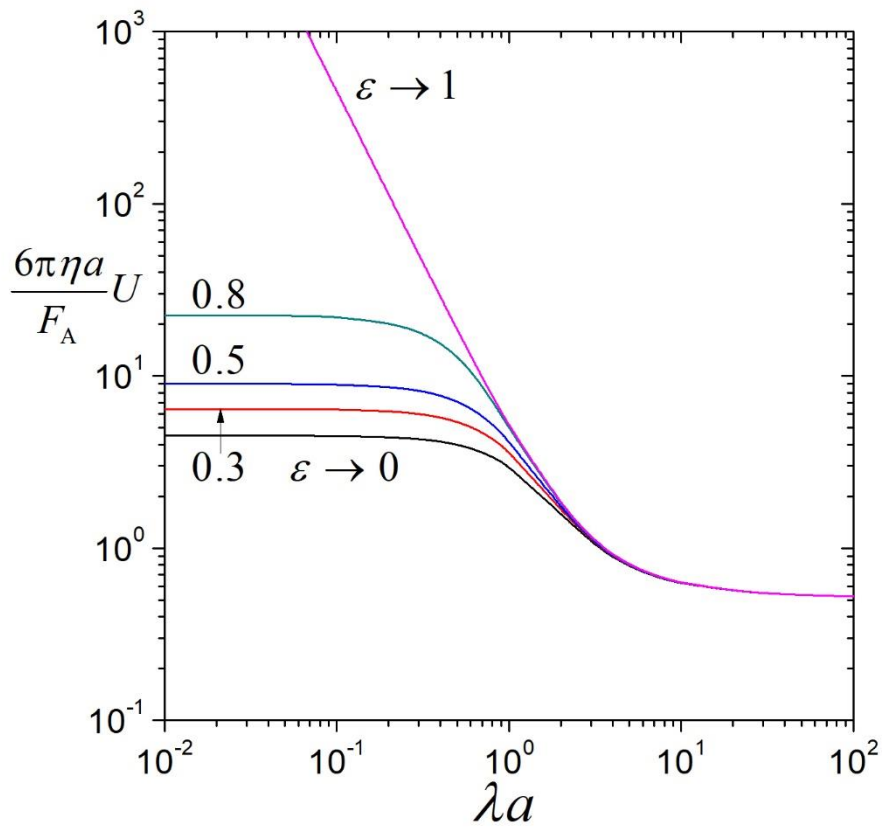
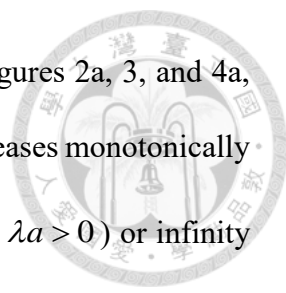


Figure 4b. The scaled particle mobility $\frac{6\pi\eta a U}{F_A}$ at $vt/a^2 = 1$ versus the shielding parameter λa with $\rho_p/\rho = 1$.



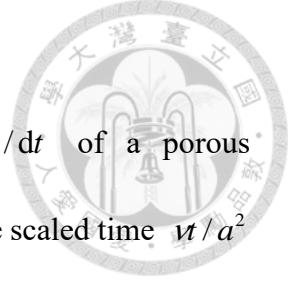
For specified values of $\nu t/a^2$, λa , and ε , as illustrated in figures 2a, 3, and 4a, the scaled velocity $6\pi\eta aU/F_A$ of the porous spherical particle decreases monotonically with an increase in the density ratio ρ_p/ρ from a finite value (as $\lambda a > 0$) or infinity (for the fully permeable case $\lambda a = 0$) at $\rho_p/\rho = 0$, indicating that a particle with greater mass density lags behind a particle with smaller density in the growth of the particle mobility. For the limiting case of $\rho_p/\rho \rightarrow \infty$, the particle velocity disappears except for the singular (steady) state $\nu t/a^2 \rightarrow \infty$. In the limit of maximum porosity $\varepsilon \rightarrow 1$, the particle velocity is independent of ρ_p/ρ .

For given values of $\nu t/a^2$, ρ_p/ρ , and ε , as illustrated in figures 2b, 3a, and 4, the scaled mobility $6\pi\eta aU/F_A$ of the porous spherical particle decreases monotonically with an increase in the shielding parameter λa from infinity (as $\nu t/a^2 \rightarrow \infty$, or $\rho_p/\rho = 0$, or $\varepsilon \rightarrow 1$) or a finite value at $\lambda a = 0$ to a smaller value for the impermeable case $\lambda a \rightarrow \infty$. When the value of λa is small, interestingly, a porous sphere with a higher fluid permeability (less λa) may develop its velocity in percentage slower relative to the reference particle toward the respective terminal values (in spite of the greater value of its velocity at any elapsed time). In the limit $\lambda a = 0$, the value of $6\pi\eta aU/F_A$ equals $9(\nu t/a^2)\rho/2(1-\varepsilon)\rho_p$, as resulting from the analytical inverse Laplace transform of equation (24) and demonstrated in figures 2b and 3a.

For fixed values of $\nu t/a^2$, ρ_p/ρ , and λa , as illustrated in figures 2c, 3b, and 4b, the scaled velocity $6\pi\eta aU/F_A$ of the porous spherical particle in general increases with an increase in the porosity ε from a finite value as $\varepsilon \rightarrow 0$ (the particle is almost impermeable) to a larger value as $\varepsilon \rightarrow 1$, indicating that a particle with smaller porosity lags behind a particle with greater porosity in the growth of the particle mobility. When

the value of ρ_p / ρ is relatively small, however, $6\pi\eta aU / F_A$ may slightly decrease with an increase in ε .

As indicated in figure 2b, the transient migration velocity of a typical porous spherical particle (say, with $\lambda a = 0.1$, $\rho_p / \rho = 1$, and $\varepsilon = 0.5$) reaches 63% of its terminal value at the scaled elapsed time $\nu t / a^2$ equal to around 50, which corresponds to a relaxation time scale of one second for a particle with $a = 0.14$ mm in water and is about 25 times of that for an impermeable solid sphere (with $\lambda a \rightarrow \infty$ and $\varepsilon = 0$). Therefore, the transient behavior of creeping motions of permeable porous particles can be much more important than that of impermeable particles. For explicit examples, the transient migration velocities of porous particles of aluminum oxide or titanium dioxide ($\rho_p / \rho = 4$) and silicon dioxide ($\rho_p / \rho = 2.5$) with $a = 1 / \lambda = 0.3$ mm and $\varepsilon = 0.5$ reach 99% of their individual terminal values at the scaled elapsed time $\nu t / a^2$ equal to 103 and 101, respectively, which correspond to slightly more than 9 seconds.



3.2 Dimensionless Particle Acceleration

Results for the dimensionless acceleration $(6\pi\rho a^3 / F_A) dU / dt$ of a porous spherical particle undergoing starting migration are plotted versus the scaled time vt / a^2 in figure 5 for various values of the density ratio ρ_p / ρ , shielding parameter λa , and porosity ε .

This acceleration is a monotonic decreasing function of vt / a^2 from a maximum at $vt / a^2 = 0$ to zero as $vt / a^2 \rightarrow \infty$. Substituting equation (24) into the initial value theorem of the Laplace transform velocity derivative $(6\pi\eta a / F_A) s\bar{U}$:

$$\lim_{s \rightarrow \infty} \left(s \cdot \frac{6\pi\eta a}{F_A} s\bar{U} \right) = \lim_{t \rightarrow 0} \left[\frac{6\pi\rho a^3}{F_A} \frac{dU}{dt} \right] = 9\rho / 2(1 - \varepsilon)\rho_p, \quad (27)$$

where the initial acceleration is independent of finite values of λa . However, substituting equation (24) with the limit $\lambda a \rightarrow \infty$ into the initial value theorem:

$$\lim_{s \rightarrow \infty} \left(s \cdot \frac{6\pi\eta a}{F_A} s\bar{U} \right) = \lim_{t \rightarrow 0} \left[\frac{6\pi\rho a^3}{F_A} \frac{dU}{dt} \right] = 9\rho [2(1 - \varepsilon)\rho_p + (1 + 2\varepsilon)\rho]^{-1}, \quad (28)$$

where the initial acceleration reveals a singular circumstance, as shown in figures 5b.

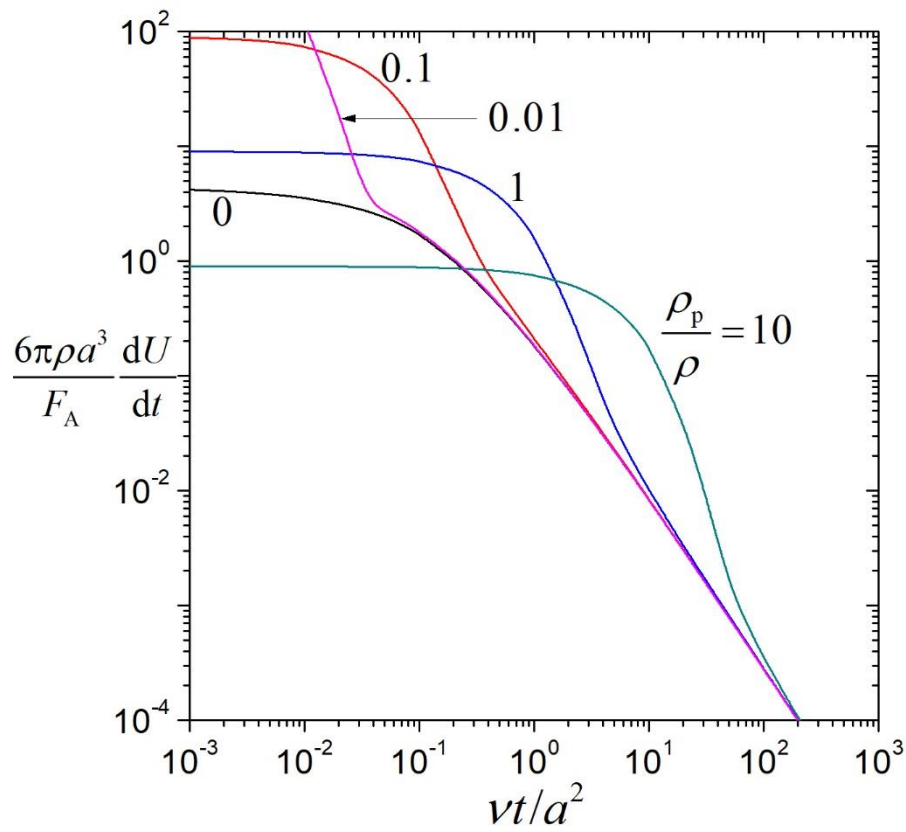
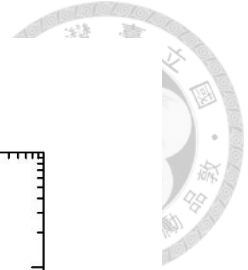


Figure 5a. The dimensionless particle acceleration $(6\pi\rho a^3 / F_A)dU / dt$ versus the dimensionless elapsed time vt/a^2 with $\lambda a = 1$ and $\varepsilon = 0.5$.

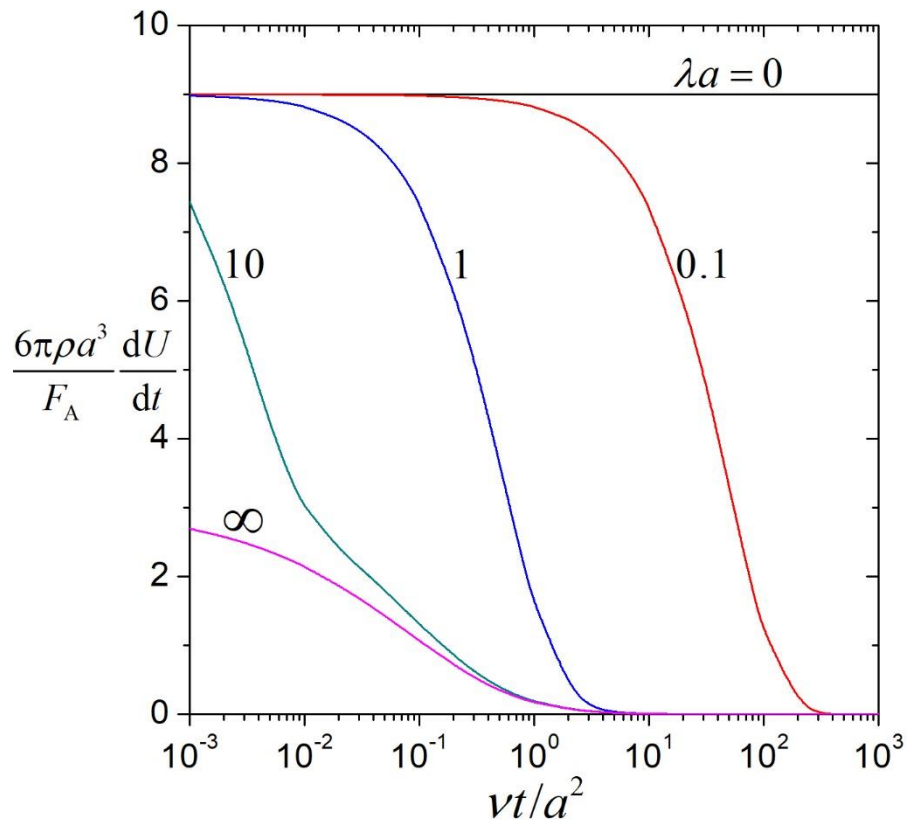
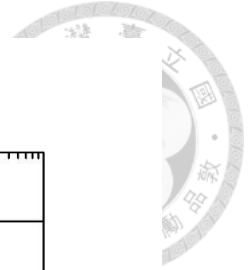


Figure 5b. The dimensionless particle acceleration $(6\pi\rho a^3/F_A)dU/dt$ versus the dimensionless elapsed time vt/a^2 with $\rho_p/\rho=1$ and $\varepsilon=0.5$.

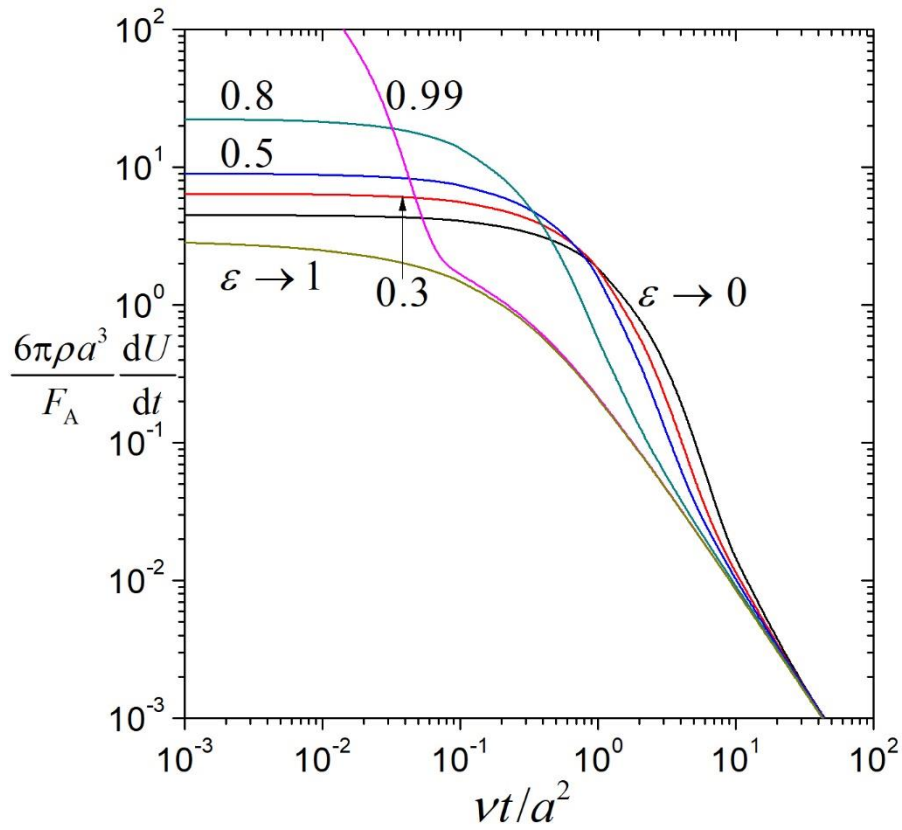
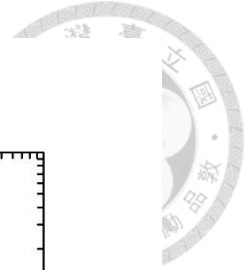
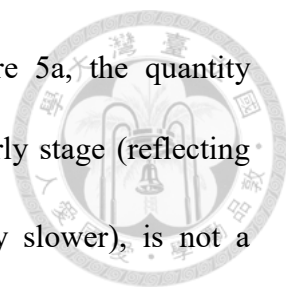


Figure 5c. The dimensionless particle acceleration $(6\pi\rho a^3 / F_A)dU / dt$ versus the dimensionless elapsed time vt/a^2 with $\lambda a = 1$ and $\rho_p / \rho = 1$.



For specified values of λa and ε , as illustrated in figure 5a, the quantity $(6\pi\rho a^3 / F_A)dU/dt$ decreases with an increase in ρ_p / ρ at the early stage (reflecting the fact that a particle with greater ρ_p / ρ develops its mobility slower), is not a monotonic function of ρ_p / ρ at the medium stage, and then increases with an increase in ρ_p / ρ at the late stage (since the particle with a small ρ_p / ρ has already developed most of its velocity to approach the steady state), but always vanishes in the limit $\rho_p / \rho \rightarrow \infty$ (where $6\pi\eta aU / F_A = 0$). In the limit of minimum density $\rho_p / \rho = 0$, as also shown in figure 2a, the initial values of $6\pi\eta aU / F_A$ and $(6\pi\rho a^3 / F_A)dU/dt$ may be $9/2\lambda^2 a^2$ and infinity, respectively, as singular circumstances at $t = 0$.

For any given values of $\nu t / a^2$, ρ_p / ρ , and ε , as shown in figure 5b, the acceleration $(6\pi\rho a^3 / F_A)dU/dt$ decreases (like the scaled velocity $6\pi\eta aU / F_A$ does) as λa increases from $9\rho / 2(1-\varepsilon)\rho_p$ at $\lambda a = 0$ [where the acceleration of the porous particle is independent of $\nu t / a^2$ and $6\pi\eta aU / F_A = 9(\nu t / a^2)\rho / 2(1-\varepsilon)\rho_p$] to a smaller value as $\lambda a \rightarrow \infty$. This outcome reflects again the behavior that a porous particle with higher fluid permeability (smaller value of λa) develops its velocity in percentage slower towards the terminal value.

For fixed values of ρ_p / ρ and λa , as illustrated in figure 5c, $(6\pi\rho a^3 / F_A)dU/dt$ increases with an increase in ε at the early stage (reflecting the fact that a particle with greater porosity develops faster), is not a monotonic function of ε at the medium stage, and then decreases with an increase in ε at the late stage (since the particle with greater porosity has already developed most of its terminal velocity). In the limit of maximum porosity $\varepsilon \rightarrow 1$, as also shown in figure 2c, the initial values of $6\pi\eta aU / F_A$ and

$(6\pi\rho a^3 / F_A)dU/dt$ may be $9/2\lambda^2 a^2$ and infinity, respectively, as singular circumstances at $t = 0$.



Chapter 4 Conclusions



In this thesis, the start-up creeping motion of a porous spherical particle in a viscous fluid produced by the sudden application of a body force is analyzed. The unsteady Stokes and Brinkman equations governing the external and internal fluid velocity distributions, respectively, about the particle are solved. A closed-form formula for the time-evolving particle velocity is obtained in Laplace transform and results of the scaled particle velocity and acceleration for various values of the scaled elapsed time $\nu t/a^2$, shielding parameter λa , relative mass density ρ_p/ρ , and porosity ε of the particle are presented. These results demonstrate that the scaled particle velocity is a monotonic increasing function of $\nu t/a^2$, a monotonic decreasing function of ρ_p/ρ and λa , and in general an increasing function of ε . Namely, a particle with greater density or smaller porosity lags behind a corresponding particle with smaller density or greater porosity in the growth of the particle mobility. On the other hand, a porous particle with a higher fluid permeability (smaller λa) may trail behind an identical particle with a lower permeability in the relative growth of the scaled mobility, although this transient mobility decreases with an increase in λa for fixed values of ρ_p/ρ and ε . The scaled acceleration of the particle decreases monotonically with increases in $\nu t/a^2$ and λa . The transient behavior of creeping motions of permeable porous particles can be much more important (with much longer relaxation time) than that of impermeable particles.

List of Symbols



a	the radius of the spherical particle, m
\mathbf{e}_z	the unit vector in the z direction, -
E^2	the axisymmetric Stokes operator, m^{-2}
f	the hydrodynamic friction coefficient per unit volume of the particle, $\text{kg} \cdot \text{m}^{-3} \cdot \text{s}^{-1}$
F_A	the applied constant force, $\text{kg} \cdot \text{m} \cdot \text{s}^{-2}$
F_h	the hydrodynamic drag on the particle, $\text{kg} \cdot \text{m} \cdot \text{s}^{-2}$
$h(r)$	the unit step function, -
\mathbf{I}	the unit dyadic, -
p	the hydrodynamic pressure profile of the fluid, $\text{kg} \cdot \text{m}^{-1} \cdot \text{s}^{-2}$
r	the radial spherical coordinate, m
s	the Laplace transform parameter, s^{-1}
t	the elapsed time, s
U	the transient migration velocity of the particle, $\text{m} \cdot \text{s}^{-1}$
U_∞	the terminal velocity of the particle, $\text{m} \cdot \text{s}^{-1}$
\mathbf{v}	the velocity distribution of the fluid, $\text{m} \cdot \text{s}^{-1}$
v_r	r component of \mathbf{v} , $\text{m} \cdot \text{s}^{-1}$
v_θ	θ component of \mathbf{v} , $\text{m} \cdot \text{s}^{-1}$



Greek letters

ε	the porosity of the particle, -
η	the viscosity of the fluid, $\text{kg} \cdot \text{m}^{-1} \cdot \text{s}^{-1}$
θ, ϕ	the angular spherical coordinates, -
$1/\lambda$	the flow penetration length or the square root of the fluid permeability in the porous particle, m
ν	the kinematic viscosity of the fluid, $\text{m}^2 \cdot \text{s}^{-1}$
ρ	the mass density of the fluid, $\text{kg} \cdot \text{m}^{-3}$
ρ_p	the mass density of the solid part of the porous particle, $\text{kg} \cdot \text{m}^{-3}$
$\boldsymbol{\tau}$	the viscous stress dyadic of the fluid, $\text{kg} \cdot \text{m}^{-1} \cdot \text{s}^{-2}$
τ_{rr}	the normal components of the viscous stress $\boldsymbol{\tau}$, $\text{kg} \cdot \text{m}^{-1} \cdot \text{s}^{-2}$
$\tau_{r\theta}$	the shear components of the viscous stress $\boldsymbol{\tau}$, $\text{kg} \cdot \text{m}^{-1} \cdot \text{s}^{-2}$
Ψ	the stream function, $\text{m}^3 \cdot \text{s}^{-1}$

References



- Abate J and Valkó P P 2004 Multi-precision Laplace transform inversion *Int. J. Numer. Meth. Eng.* 60 979–993
- Ashmawy E A 2012 A general formula for the drag on a sphere placed in a creeping unsteady micropolar fluid flow *Meccanica* 47 1903-1912
- Ashmawy E A 2017 Unsteady translational motion of a slip sphere in a viscous fluid using the fractional Navier-Stokes equation *Eur. Phys. J. Plus* 132 142
- Basset A B 1888 *A Treatise on Hydrodynamics* vol 2 (Cambridge: Deighton, Bell and Co.)
- Bird R B, Stewart W E and Lightfoot E N 2007 *Transport phenomena* revised 2nd ed. (New York: Wiley)
- Brinkman H C 1947 A calculation of the viscous force exerted by a flowing fluid on a dense swarm of particles *Appl. Sci. Res.* A1 27-34
- Buonocore S, Sen M and Semperlotti F 2019 A fractional-order approach for transient creeping flow of spheres *AIP Advances* 9 085323
- Dill L H and Balasubramaniam R 1992 Unsteady thermocapillary migration of isolated drops in creeping flow *Int. J. Heat Fluid Flow* 13 78-85
- Fakour M, Rahbari A, Moghadasi H, Rahimipetroudi I, Domairry Ganji D and Varmazyar M 2018 Analytical study of unsteady sedimentation analysis of spherical particle in Newtonian fluid media *Thermal Sci.* 22 847-855
- Feng J and Joseph D D 1995 The unsteady motion of solid bodies in creeping flows *J. Fluid Mech.* 303 83-102
- Gomez-Solano J R and Bechinger C 2015 Transient dynamics of a colloidal particle driven through a viscoelastic fluid *New J. Phys.* 17 103032
- Hadamard J S 1911 Mouvement permanent lent d'une sphere liquid et visqueuse dans un

liquide visqueux *Compt. Rend. Acad. Sci. (Paris)* 152 1735-1738



Keh H J and Huang Y C 2005 Transient electrophoresis of dielectric spheres *J. Colloid*

Interface Sci. 291 282-291

Lai Y C and Keh H J 2020 Transient electrophoresis of a charged porous particle

Electrophoresis 41 259-265

Lai Y C and Keh H J 2021 Transient electrophoresis in a suspension of charged particles

with arbitrary electric double layers *Electrophoresis* 42 2126-2133

Li M X and Keh H J 2020 Start-up electrophoresis of a cylindrical particle with arbitrary

double layer thickness *J. Phys. Chem. B* 124 9967-9973.

Li M X and Keh H J 2021 Transient rotation of a spherical particle in a concentric cavity

with slip surfaces *Fluid Dyn. Res.* 53 045509

Liu Y C and Keh H J 1998 Sedimentation velocity and potential in a dilute suspension of

charged porous spheres *Colloids Surfaces A* 140 245-259

Masliyah J H and Polikar M 1980 Terminal velocity of porous spheres *Can. J. Chem. Eng.*

58 299-302

Matsumoto K and Sukanuma A 1977 Settling velocity of a permeable model floc *Chem.*

Eng. Sci. 32 445-447

Michaelides E E 1997 Review-The transient equation of motion for particles, bubbles,

and droplets *J. Fluids Eng.* 119 233-247

Morrison F A and Reed L D 1975 Unsteady creeping motion of a sphere at small values

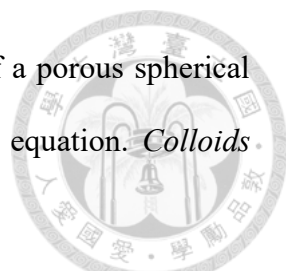
of Knudsen number *J. Aerosol Sci.* 6 9-18

Neale G, Epstein N and Nader W 1973 Creeping flow relative to permeable spheres *Chem.*

Eng. Sci. 28 1865-1874

Prakash J and Raja Sekhar G P 2012 Arbitrary oscillatory Stokes flow past a porous

sphere using Brinkman model *Meccanica* 47 1079-1095

- 
- Prakash J and Satyanarayana C 2021 Axisymmetric slow motion of a porous spherical particle in a viscous fluid using time fractional Navier–Stokes equation. *Colloids Interfaces* 5 24
- Premlata A R and Wei H-H 2020 Re-entrant history force transition for stick-slip Janus swimmers: mixed Basset and slip-induced memory effects *J. Fluid Mech.* 882 A7
- Rybczynski W 1911 Uber die fortschreitende bewegung einer flussigen kugel in einem zahnmedium *Bull. Acad. Sci., Cracovie, Ser. A* 1 40-46
- Sharanya V and Raja Sekhar G P 2015 Thermocapillary migration of a spherical drop in an arbitrary transient Stokes flow *Phys. Fluids* 27 063104
- Stehfest H 1970 Algorithm 368 Numerical inversion of Laplace transforms *Comm. ACM* 13 47-49
- Stewart M B and Morrison F A 1981 Droplet dynamics in creeping flows *J. Appl. Mech.* 48 224-228
- Stokes G G 1851 On the effect of the internal friction of fluid on pendulums *Trans. Cambridge Philos. Soc.* 9 8-106
- Sutherland D N and Tan C T 1970 Sedimentation of a porous sphere *Chem. Eng. Sci.* 25 1948-1950
- Yossifon G, Frankel I and Miloh T 2009 Macro-scale description of transient electrokinetic phenomena over polarizable dielectric solids *J. Fluid Mech.* 620 241-262

Appendix A

Start-up Rotation of a Porous Sphere in a Cavity



A.1 Introduction

The translation and rotation of solid particles in viscous fluids at low Reynolds numbers play important roles in a variety of technological and industrial processes such as sedimentation, centrifugation, agglomeration, microfluidics, suspension rheology, aerosol technology, and motion of blood cells in arteries and veins. The analytical study of this topic grew out of the classic work of Stokes [1,2] on the steady motion of an isolated hard sphere in an incompressible Newtonian fluid.

Some small particles are porous, viz. permeable to fluids, such as macromolecules and flocs of fine particles. The translational and rotational motions of porous particles have been extensively studied for decades. An approach which comprises a second-order viscous term to Darcy's equation for fluid flow through porous media was established by Brinkman [3]. Neale et al. [4] analyzed the translation of a porous sphere by using the Brinkman equation for the internal flow and the Stokes equation for the external flow with appropriate boundary conditions on the particle surface and the assumption that the effective viscosity inside the porous sphere equals the bulk fluid viscosity. Matsumoto and Suganuma [5] and Masliyah and Polikar [6] experimentally investigated the sedimentation of porous particles, the results of which agree well with the analytical formula obtained by Neale et al. [4].

The angular velocity of a porous sphere of radius a rotating under an applied torque T_A about its diameter in an unbounded fluid of viscosity η at the steady state of low Reynolds numbers has been obtained by solving the Brinkman and Stokes equations, with the result [7]

$$\Omega_\infty = \frac{T_A}{8\pi\eta a^3 \omega}, \quad (\text{A1})$$

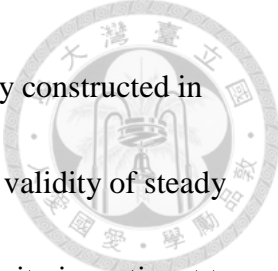
$$\omega = 1 + \frac{3}{(\lambda a)^2} - \frac{3}{\lambda a} \coth(\lambda a), \quad (\text{A2})$$

where λ^{-1} is the flow penetration length of the porous particle. In the limits $\lambda a = 0$ (fully permeable in the porous particle) and $\lambda a \rightarrow \infty$ (impermeable), Eq. (A1) results in $\Omega_\infty \rightarrow \infty$ ($\omega = 0$) and $\Omega_\infty = T_A / 8\pi\eta a^3$ ($\omega = 1$, Stokes' result for a hard sphere), respectively.

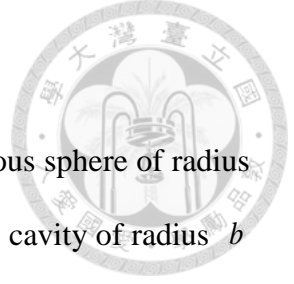
Particles move in bounded fluids in real situations, so it is important to know whether the proximity of a boundary affects the rotation of particles significantly [8-13]. In the operation of rotational viscometers and stirred vessels for high-viscosity liquids, it is necessary to determine the relationship between angular velocity and torque as the confining boundary is approached. The steady low-Reynolds-number rotation of a porous sphere about its diameter at the center of a spherical cavity was analytically studied, with the particle's angular velocity given by [7,14]

$$\Omega_\infty = \frac{T_A}{8\pi\eta a^3 \omega} \left(1 - \frac{a^3}{b^3} \omega\right), \quad (\text{A3})$$

where b is the radius of the cavity. When $a/b = 0$, the previous equation becomes Eq. (A1). Recently, the rotational motions of a porous sphere about its diameter at low Reynolds numbers within an approximate or eccentric spherical cavity [15-18] and near other boundaries [19,20] were also analyzed.



Although the basic formulation of slow particle rotation is mainly constructed in steady state, its transient behavior is also important for evaluating the validity of steady supposition [21,22]. The temporal evolution of particle's angular velocity is pertinent to particle dynamics in the sub-millisecond range [23,24]. The low-Reynolds-number response of the torques exerted by the fluid on isolated hard and soft particles to unsteady rotation has been studied to some extent [25-27]. Recently, the transient rotation of a hard particle caused by a suddenly applied torque in a confining cavity was also investigated [28]. However, the starting rotation of isolated or confined porous particles has not been examined. Knowledge of the start-up rotation in the proximity of confining boundaries may be important, for example, in the rotational viscometers and agitated vessels for highly viscous liquids. In this appendix, the initial rotation of a porous sphere because of the sudden application of a continuous torque about its diameter at the center of a spherical cavity is analyzed. An explicit expression is obtained for the temporal Laplace transform of the transient angular velocity of the porous sphere.



A.2 Analysis

As shown in Fig. A1, we consider the start-up rotation of a porous sphere of radius a about its diameter in a viscous fluid within a concentric spherical cavity of radius b in the spherical coordinate system (r, θ, ϕ) . At time $t=0$, the constant torque T_A in the z direction (about the axis $\theta=0$) is suddenly applied to the originally motionless porous sphere and continues thereafter. The transient angular velocity $\Omega(t)$ (also in the z direction) of the particle, which is zero at $t=0$ and equals the steady value Ω_∞ given by Eq. (A3) as $t \rightarrow \infty$, needs to be determined. The angular Reynolds number $Re = \Omega_\infty a^2 / \nu$ is vanishingly small, where ν is the kinematic viscosity of the fluid.

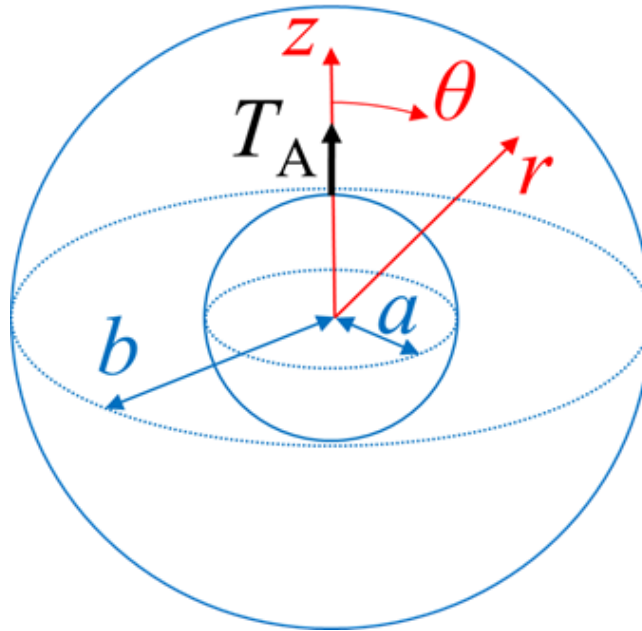


Figure A1. Geometric sketch for a porous sphere of radius a rotating under the applied torque T_A in the z direction within a concentric cavity of radius b in the spherical coordinate system (r, θ, ϕ) .



The velocity \mathbf{v} and hydrodynamic pressure p of the fluid are governed by the transient Stokes and Brinkman equations,

$$[1-h(r)(1-\varepsilon)]\rho \frac{\partial \mathbf{v}}{\partial t} = -\nabla p + \eta \nabla^2 \mathbf{v} - h(r)\eta \lambda^2 (\mathbf{v} - \boldsymbol{\Omega} \times r \mathbf{e}_r), \quad (\text{A4})$$

where $\boldsymbol{\Omega} = \Omega(t)\mathbf{e}_z$ is the angular velocity of the porous sphere (equal to zero at $t = 0$) to be determined, \mathbf{e}_r and \mathbf{e}_z are unit vectors in the r and z directions, respectively, ρ and η are the mass density and viscosity, respectively, of the fluid, ε and λ^{-1} are the porosity and flow penetration length or square root of the fluid permeability, respectively, of the particle, $h(r)$ is a step function equal to unity if $r \leq a$ and zero otherwise. λ^{-1} is proportional to $\varepsilon^{3/2} / (1-\varepsilon)$ and the pore size according to the Blake-Kozeny equation [29]. In the Brinkman equation [i.e., Eq. (A4) for $r \leq a$], \mathbf{v} is the superficial velocity averaged over a region of space of the solid plus fluid, large with respect to the pore size, but small with respect to the particle radius a , the last term relates to the friction force between internal sphere flow and rigid sphere backbone, and the viscosity η is assumed to be the bulk phase value [4].

For the transient rotation of a porous sphere about its diameter in a viscous fluid within a concentric spherical cavity, Eq. (A4) can be written as

$$[1-h(r)(1-\varepsilon)] \frac{r^2}{v} \frac{\partial v_\phi}{\partial t} = \frac{\partial}{\partial r} \left(r^2 \frac{\partial v_\phi}{\partial r} \right) + \frac{\partial}{\partial \theta} \left[\frac{1}{\sin \theta} \frac{\partial}{\partial \theta} (v_\phi \sin \theta) \right] - h(r)\lambda^2 r^2 (v_\phi - \Omega r \sin \theta), \quad (\text{A5})$$

where $v_\phi(r, \theta, t)$ is the azimuthal (only nonzero) component of the fluid velocity satisfying the continuity equation and the hydrodynamic pressure is a constant throughout the space in the limit of low Reynolds number.



The initial and boundary conditions are

$$t = 0: \quad v_\phi = 0, \quad (A6)$$

$$r = 0: \quad v_\phi \text{ is finite}, \quad (A7)$$

$$r = a: \quad v_\phi \text{ and } \tau_{r\phi} \text{ are continuous}, \quad (A8)$$

$$r = b: \quad v_\phi = 0, \quad (A9)$$

where $\tau_{r\phi}$ is the only nonzero shear stress of the fluid at the particle surface. Equations (A7)-(A9) express the absence of any velocity field singularity, the continuity of velocity and hydrodynamic stress fields at the particle surface, and stick (zero-slip) condition at the stationary inner container surface, respectively.

Equations (A5)-(A9) suggest the form of the fluid velocity to be

$$v_\phi = g(r, t) \sin \theta, \quad (A10)$$

The Laplace transform, which is defined by an over-bar for a function of time $f(t)$ as

$$\bar{f}(s) = \int_0^\infty f(t) \exp(-st) dt, \quad (A11)$$

$$f(t) = \frac{1}{2\pi i} \int_{\gamma-i\infty}^{\gamma+i\infty} \bar{f}(s) \exp(st) ds, \quad (A12)$$

will be used to solve for the flow field and particle' angular velocity. Then, the transform of Eqs. (A5) and (A10) can be expressed as

$$\left\{ \frac{d^2}{dr^2} + \frac{2}{r} \frac{d}{dr} - \frac{2}{r^2} - h(r)\lambda^2 - [1 - h(r)(1 - \varepsilon)] \frac{s}{v} \right\} \bar{g}(r, s) = -h(r)\lambda^2 r \bar{\Omega}(s), \quad (A13)$$

where s is the transform variable.

The general solution of Eq. (A13) that satisfies the initial condition (A6) is

$$\bar{v}_\phi = \bar{\Omega}a[C_1 I_{3/2}(Ar) + C_2 I_{-3/2}(Ar)](Ar)^{-1/2} \sin \theta \quad (\text{A14})$$

$$\bar{v}_\phi = \bar{\Omega}r\left\{\left(\frac{\lambda}{B}\right)^2 + [(C_3 + C_4 Br) \cosh(Br) - (C_3 Br + C_4) \sinh(Br)]\left(\frac{a}{r}\right)^3\right\} \sin \theta \quad \text{if } r \leq a, \quad (\text{A15})$$

where $A = \sqrt{s/\nu}$, $B = \sqrt{\lambda^2 + \varepsilon s/\nu}$, and I_n are the modified Bessel functions of the first kind. The unknown constants (functions of s actually) C_1 , C_2 , C_3 , and C_4 are determined from the boundary conditions (A7)-(A9) as

$$C_1 = \sqrt{\frac{\pi}{2}} \left(\frac{\lambda}{B}\right)^2 L_1 L_3 G, \quad (\text{A16})$$

$$C_2 = \sqrt{\frac{\pi}{2}} \left(\frac{\lambda}{B}\right)^2 L_2 L_3 G, \quad (\text{A17})$$

$$C_3 = 0, \quad (\text{A18})$$

$$C_4 = \left(\frac{\lambda}{B}\right)^2 L_4 G, \quad (\text{A19})$$

where

$$G = [L_5 \sinh(Ba) - L_6 \cosh(Ba)]^{-1}, \quad (\text{A20})$$

$$L_1 = A^2 a^2 [Ab \sinh(Ab) - \cosh(Ab)], \quad (\text{A21})$$

$$L_2 = A^2 a^2 [\sinh(Ab) - Ab \cosh(Ab)], \quad (\text{A22})$$

$$L_3 = (3 + B^2 a^2) \sinh(Ba) - 3Ba \cosh(Ba), \quad (\text{A23})$$

$$L_4 = \cosh(Aa)[N_1 \cosh(Ab) + N_2 \sinh(Ab)] - \sinh(Aa)[N_2 \cosh(Ab) + N_1 \sinh(Ab)], \quad (\text{A24})$$

$$L_5 = \cosh(Aa)[N_3 \cosh(Ab) + N_4 \sinh(Ab)] - \sinh(Aa)[N_4 \cosh(Ab) + N_3 \sinh(Ab)], \quad (\text{A25})$$



$$L_6 = Ba[L_1 \sinh(Aa) + L_2 \cosh(Aa)], \quad (A26)$$

$$N_1 = Aa(3 - A^2 ab) - 3Ab, \quad (A27)$$

$$N_2 = 3 - A^2 a(3b - a), \quad (A28)$$

$$N_3 = AB^2 a^2 (b - a) - A^3 a^2 b, \quad (A29)$$

$$N_4 = A^2 a^2 (1 + B^2 ab) - B^2 a^2, \quad (A30)$$

The torque exerted by the fluid on the particle (in the z direction) is negative and its Laplace transform is given by

$$\bar{T}_h = 2\pi\eta\lambda^2 \int_0^\pi \int_0^a (\bar{v}_\phi - \bar{\Omega}r\sin\theta)r^3 \sin^2\theta dr d\theta, \quad (A31)$$

whose magnitude increases monotonically with the elapsed time from naught at $t = 0$ to T_A as $t \rightarrow \infty$. By using Eq. (A5) and the Gauss divergence theorem, Eq. (A31) can also be expressed as

$$\bar{T}_h = 2\pi a^3 \int_0^\pi \bar{\tau}_{r\phi}(r = a) \sin^2\theta d\theta - 2\pi\varepsilon\rho_s \int_0^\pi \int_0^a \bar{v}_\phi r^3 \sin^2\theta dr d\theta, \quad (A32)$$

The substitution of Eqs. (A14)-(A19) into Eq. (A31) or (A32) leads to

$$\bar{T}_h = \frac{8}{15}\pi\eta a^3 \bar{\Omega} \{ \lambda^2 a^2 [(\frac{\lambda}{B})^2 - 1] + 5(\frac{\lambda}{B})^2 L_3 L_4 G \}, \quad (A33)$$

where η is the viscosity of the fluid. Note that v_ϕ and T_h vanish in the limiting case of $\lambda a = 0$.

The sum of the applied and hydrodynamic torques on the particle equals the angular acceleration multiplied by the moment of inertia,

$$T_h + T_A = \frac{8}{15}\pi a^5 (1 - \varepsilon) \rho_p \frac{d\Omega}{dt}, \quad (A34)$$

where ρ_p is the mass density of the solid part of the porous sphere.



Substitution of Eq. (A33) into Eq. (A34) results in a formula for the transient angular velocity of the porous sphere in transform,

$$\bar{\Omega} = \frac{15T_A}{8\pi\eta a^3 s} \left\{ A^2 a^2 (1-\varepsilon) \frac{\rho_p}{\rho} - 5 \left(\frac{\lambda}{B}\right)^4 L_3 L_4 G + \lambda^2 a^2 \left[1 - \left(\frac{\lambda}{B}\right)^2\right] \right\}^{-1}, \quad (\text{A35})$$

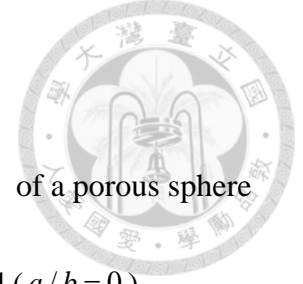
where $\rho = \eta / \nu$ is the density of the fluid. This angular velocity can be obtained numerically using the inverse Laplace transform [30,31]. In the limiting case of $\lambda a \rightarrow \infty$ (the porous sphere becomes impermeable with $\varepsilon = 0$), Eq. (A35) is identical to the corresponding formula obtained for the transient rotation of a hard sphere inside a spherical cavity taking the surfaces to be nonslip [28].

If the applied torque T_A is suddenly taken away from a rotating porous sphere that is already at a steady state with angular velocity Ω_∞ , the transient angular velocity of the porous sphere that stops rotating will decay from Ω_∞ to zero as $\Omega_\infty - \Omega$ decreases with time calculated using the inverse transform of Eq. (A35).

In the limit $a/b=0$, $L_4 G$ in Eq. (A35) reduces to that for the porous sphere rotating in an unbounded fluid:

$$L_4 G = - \frac{3 + 3Aa + A^2 a^2}{A^2 B a^3 \cosh(Ba) + (AB^2 a - A^2 + B^2) a^2 \sinh(Ba)}. \quad (\text{A36})$$

A.3 Results and Discussion



The nondimensionalized starting angular velocity $8\pi\eta a^3\Omega/T_A$ of a porous sphere applied by constant torque T_A about a diameter in a boundless fluid ($a/b=0$) calculated from Eqs. (A35) and (A36) by means of numerical inverse transform is plotted versus the dimensionless passed time $\nu t/a^2$, relative density ρ_p/ρ , shielding parameter λa , and porosity ε of the particle in Figs. A2-A4. For fixed values of λa , ρ_p/ρ , and ε , as expected, the particle's angular velocity grows continuously with $\nu t/a^2$ from zero at $\nu t/a^2=0$ to the final rate given by Eq. (A1) (which does not depend on ρ_p/ρ or ε) as $\nu t/a^2 \rightarrow \infty$. In the limits of minimum density $\rho_p/\rho=0$ and maximum porosity $\varepsilon \rightarrow 1$ of the particle, as shown in Figs. A2a and A2c, the initial value of $8\pi\eta a^3\Omega/T_A$ may also be $15/\lambda^2 a^2$ as singular situations at $t=0$.

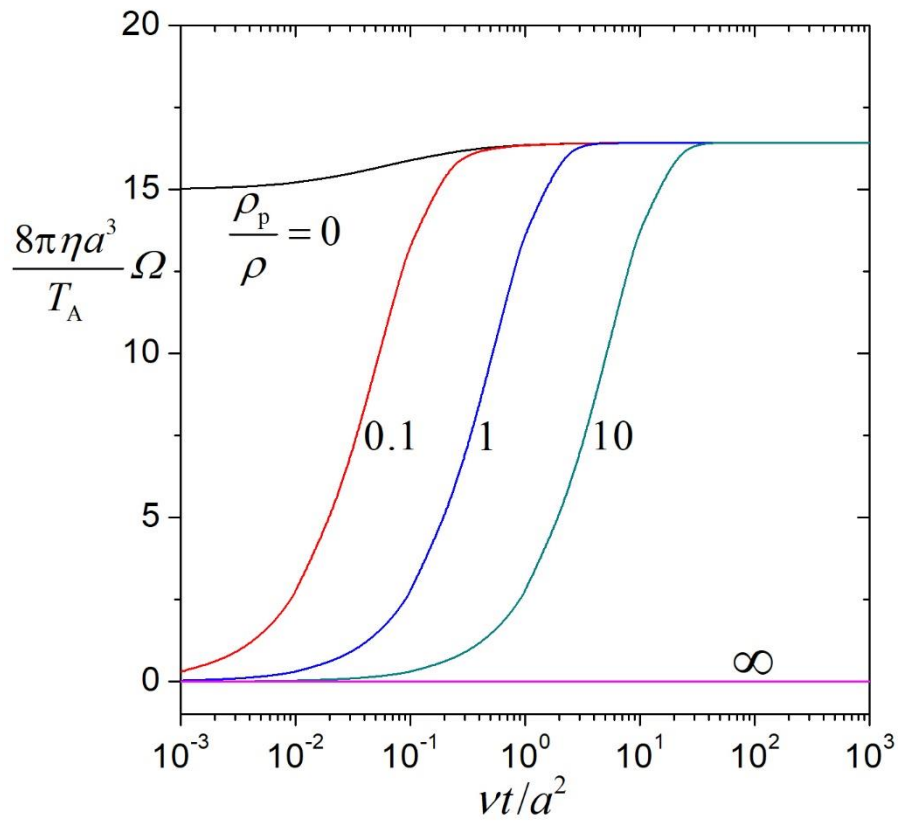


Figure A2a. Dimensionless angular velocity $8\pi\eta a^3\Omega/T_A$ of a spherical porous particle in a boundless fluid versus the dimensionless elapsed time vt/a^2 with $\lambda a = 1$ and $\varepsilon = 0.5$.

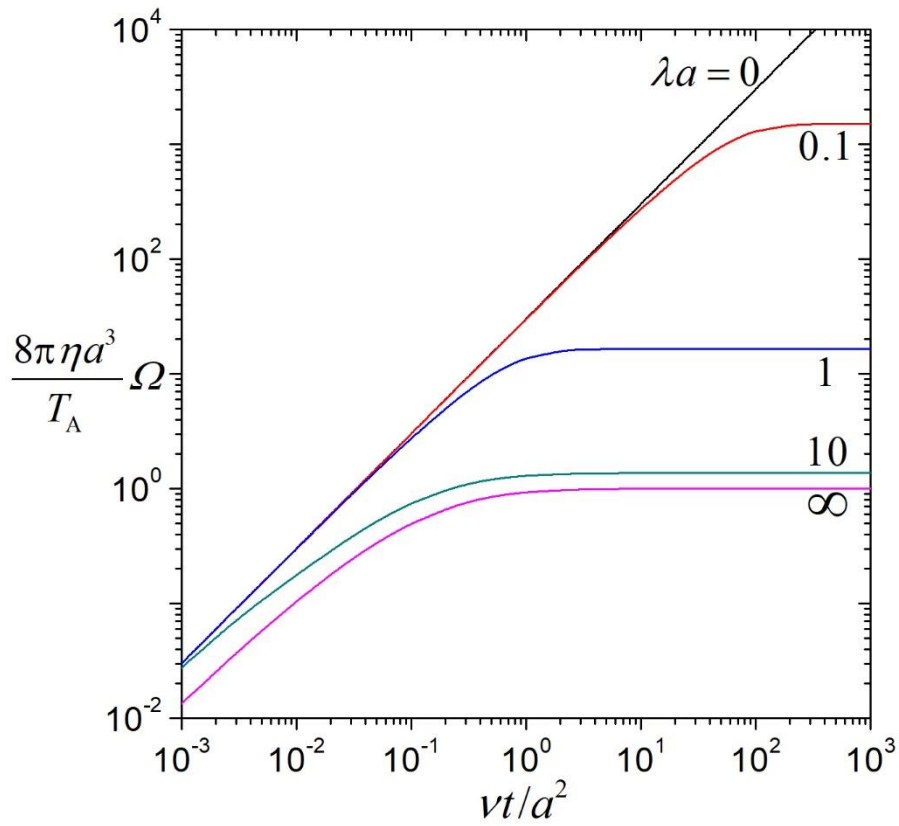


Figure A2b. Dimensionless angular velocity $\frac{8\pi\eta a^3 \Omega}{T_A}$ of a spherical porous particle in a boundless fluid versus the dimensionless elapsed time vt/a^2 with $\rho_p/\rho=1$ and $\varepsilon=0.5$.

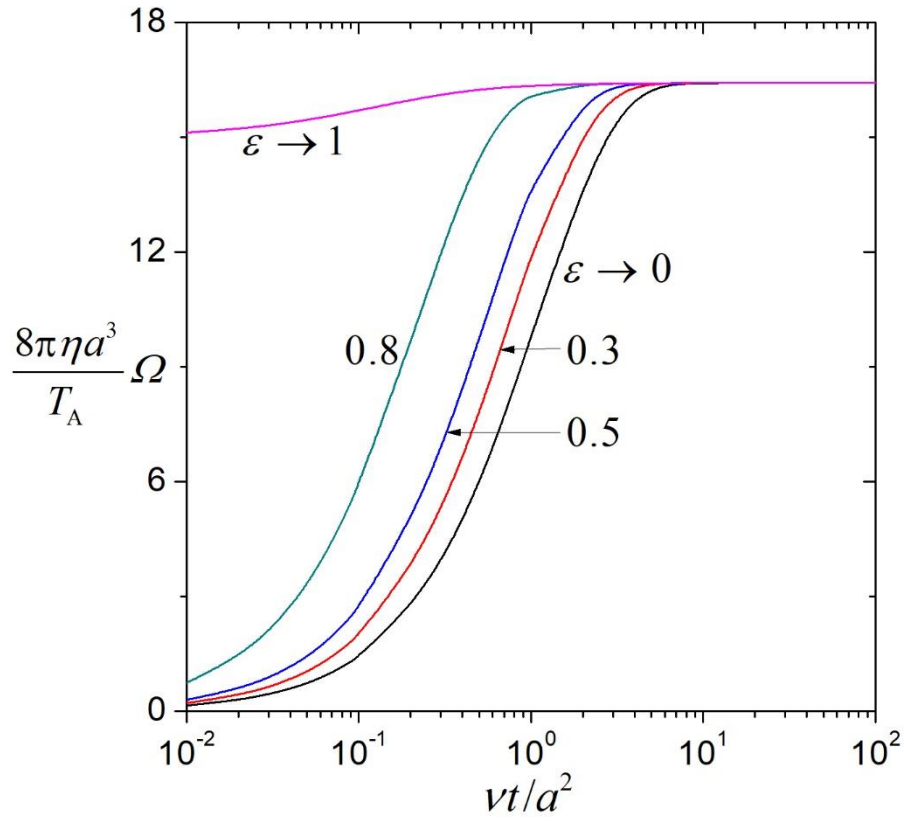


Figure A2c. Dimensionless angular velocity $\frac{8\pi\eta a^3 \Omega}{T_A}$ of a spherical porous particle in a boundless fluid versus the dimensionless elapsed time vt/a^2 with $\lambda a = 1$ and $\rho_p / \rho = 1$.

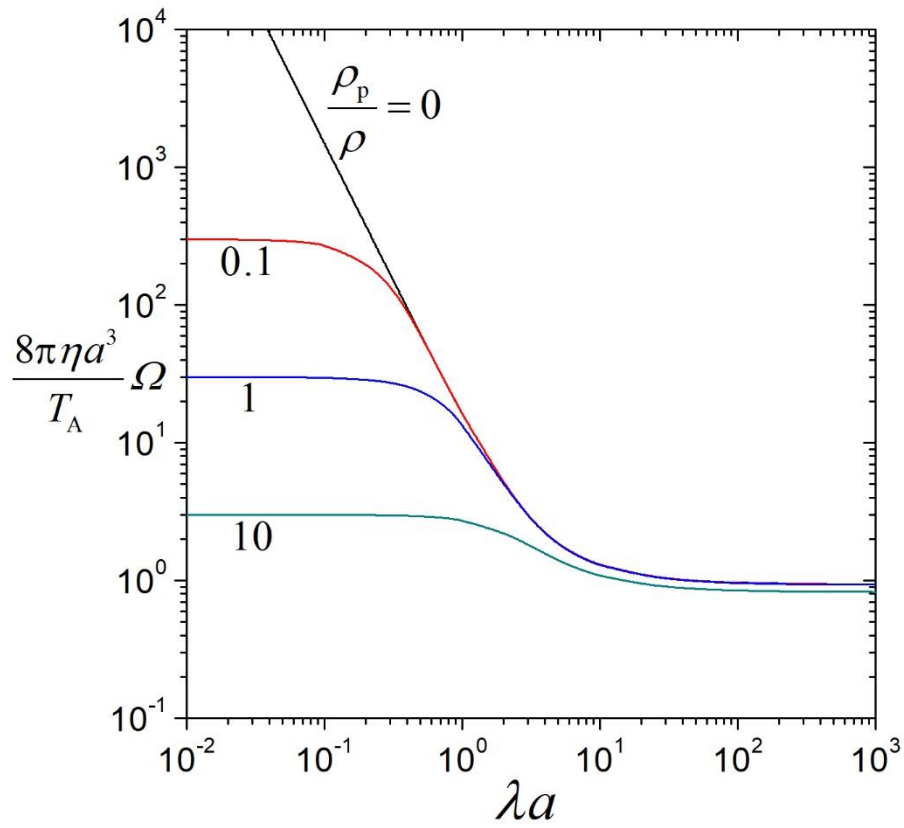


Figure A3a. Dimensionless angular velocity $8\pi\eta a^3 \Omega / T_A$ of a spherical porous particle in a boundless fluid at $vt/a^2 = 1$ versus the shielding parameter λa with $\varepsilon = 0.5$.

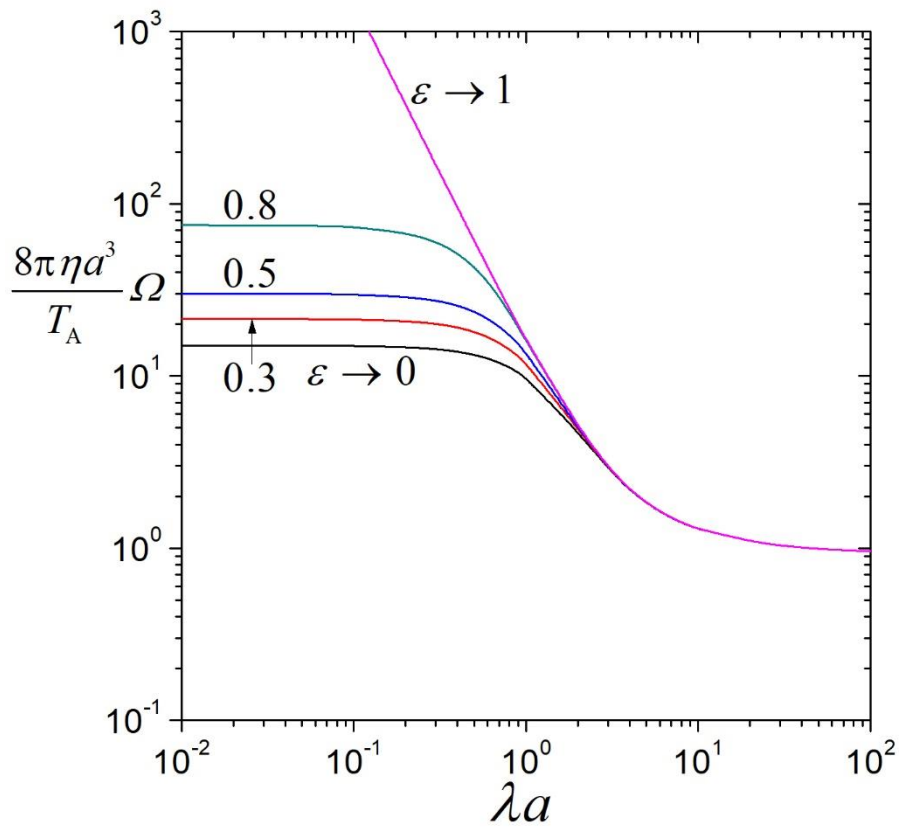


Figure A3b. Dimensionless angular velocity $8\pi\eta a^3 \Omega / T_A$ of a spherical porous particle in a boundless fluid at $vt/a^2 = 1$ versus the shielding parameter λa with $\rho_p / \rho = 1$.

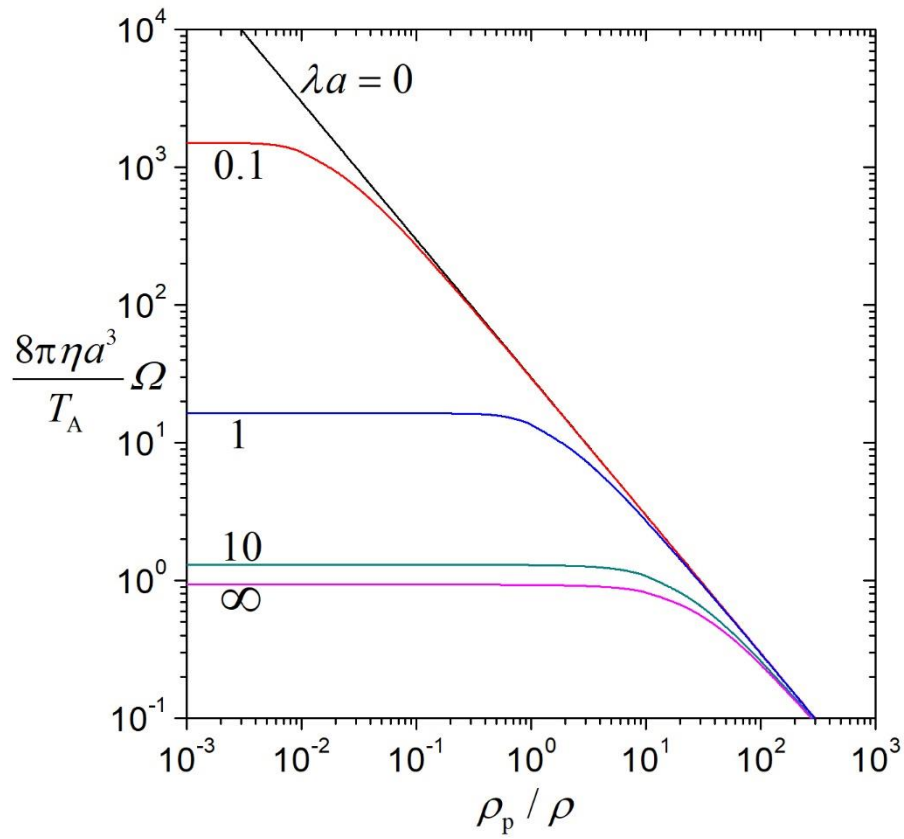
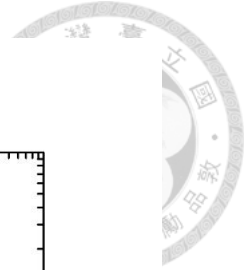


Figure A4a. Dimensionless angular velocity $8\pi\eta a^3 \Omega / T_A$ of a spherical porous particle in a boundless fluid at $vt/a^2 = 1$ versus the density ratio ρ_p / ρ with $\varepsilon = 0.5$.

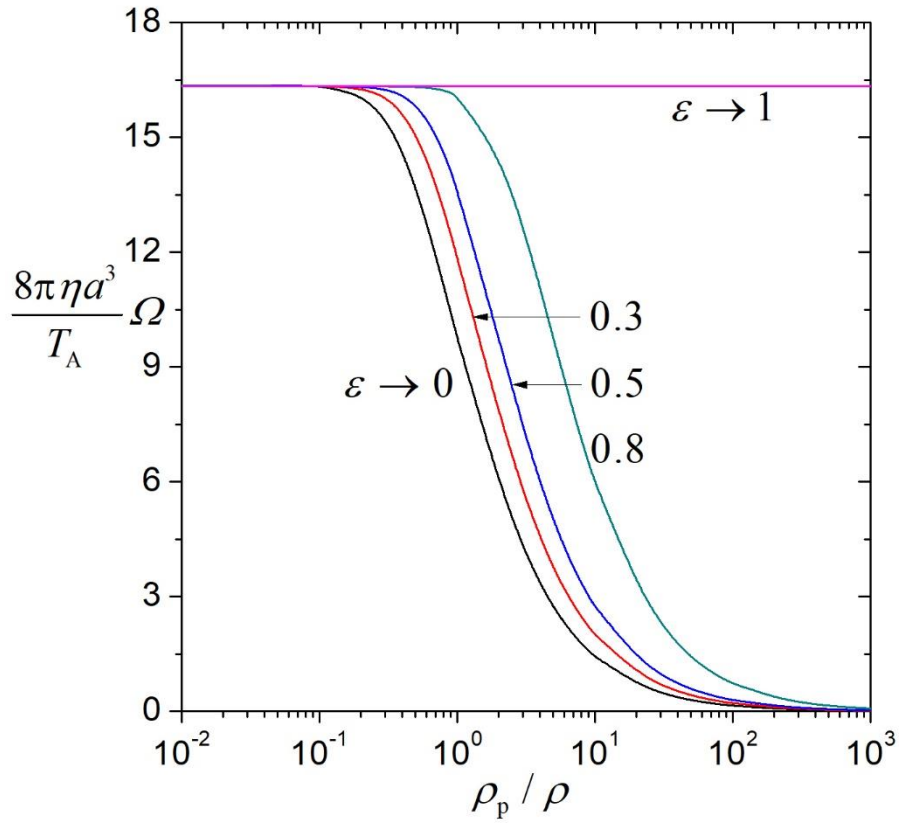
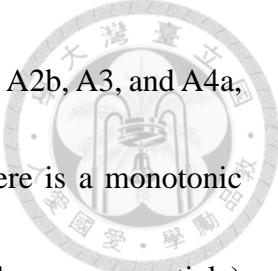
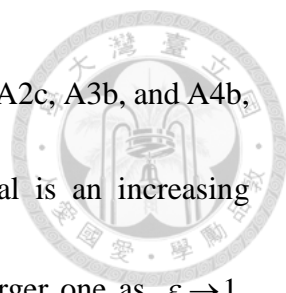


Figure A4b. Dimensionless angular velocity $8\pi\eta a^3\Omega/T_A$ of a spherical porous particle in a boundless fluid at $vt/a^2=1$ versus the density ratio ρ_p/ρ with $\lambda a=1$.



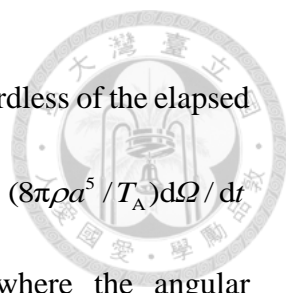
For specified values of vt/a^2 , ρ_p/ρ , and ε , as shown in Figs. A2b, A3, and A4a, the dimensionless angular velocity $8\pi\eta a^3\Omega/T_A$ of the porous sphere is a monotonic decreasing function of λa (relative resistance to fluid flow inside the porous particle) from infinity (as $vt/a^2 \rightarrow \infty$, or $\rho_p/\rho = 0$, or $\varepsilon \rightarrow 1$) or a finite value at $\lambda a = 0$ (fully permeable particle) to a smaller value as $\lambda a \rightarrow \infty$ (impermeable particle), illustrating the reduction in the transient angular velocity of the porous particle with an increase in its internal resistance to fluid flow at any elapsed time. When the value of λa is small, interestingly, a porous particle with higher fluid permeability (smaller value of λa) develops its angular velocity in percentage slower relative to the reference particle towards the respective terminal values (despite the greater value of its angular velocity at any elapsed time). In the limit $\lambda a = 0$, the value of $8\pi\eta a^3\Omega/T_A$ equals $15(vt/a^2)\rho/(1-\varepsilon)\rho_p$, as resulting from equation (A35).

For fixed values of vt/a^2 , λa , and ε , as illustrated in Figs. A2a, A3a, and A4, the angular velocity $8\pi\eta a^3\Omega/T_A$ is a monotonic decreasing function of the density ratio ρ_p/ρ from a finite value (as $\lambda a > 0$) or infinity (for the completely permeable case $\lambda a = 0$) at $\rho_p/\rho = 0$, indicating the diminution in the transient angular velocity of the particle with an increase in its relative density. In the limit $\rho_p/\rho \rightarrow \infty$, the angular velocity vanishes except for the steady state $vt/a^2 \rightarrow \infty$. For the limiting case of maximum porosity $\varepsilon \rightarrow 1$, the angular velocity does not depend on ρ_p/ρ .



For given values of $\nu t/a^2$, ρ_p/ρ , and λa , as shown in Figs. A2c, A3b, and A4b, the angular velocity $8\pi\eta a^3\Omega/T_A$ of the porous sphere in general is an increasing function of the porosity ε from a finite value as $\varepsilon \rightarrow 0$ to a larger one as $\varepsilon \rightarrow 1$, illustrating that a particle with smaller porosity lags behind that with greater porosity in the development of the angular velocity. However, $8\pi\eta a^3\Omega/T_A$ may slightly decrease with an increase in ε when the value of ρ_p/ρ is relatively small.

The dimensionless angular acceleration $(8\pi\rho a^5/T_A)d\Omega/dt$ of a porous sphere starting to rotate under the application of a constant torque in a boundless fluid as a function of the dimensionless time $\nu t/a^2$ is presented in Fig. A5 for various values of the shielding parameter λa , density ratio ρ_p/ρ , and porosity ε . This angular acceleration decreases monotonically with an increase in $\nu t/a^2$ from a maximum equal to $15\rho/(1-\varepsilon)\rho_p$ (independent of finite values of λa) or $15\rho/[(1-\varepsilon)\rho_p + \varepsilon\rho]$ (for the singular limit $\lambda a \rightarrow \infty$) at $\nu t/a^2 = 0$ and disappears as $\nu t/a^2 \rightarrow \infty$. For given values of λa and ε , the angular acceleration $(8\pi\rho a^5/T_A)d\Omega/dt$ decreases as ρ_p/ρ increases at the early stage, is not a monotonic function of ρ_p/ρ at the medium stage, and then increases with an increase in ρ_p/ρ at the late stage, but always vanishes in the limit $\rho_p/\rho \rightarrow \infty$ (where $8\pi\eta a^3\Omega/T_A = 0$). This consequence reproduces the fact that a particle of higher relative density grows its angular velocity slower but has the terminal value independent of the relative density. In the limiting case of $\rho_p/\rho \rightarrow \infty$, the angular



acceleration of the particle vanishes (so does its angular velocity) regardless of the elapsed time. For any fixed values of vt/a^2 , ρ_p/ρ , and ε , the quantity $(8\pi\rho a^5/T_A)d\Omega/dt$ decreases as λa increases from $15\rho/(1-\varepsilon)\rho_p$ at $\lambda a=0$ [where the angular acceleration of the porous sphere does not depend on the elapsed time and $8\pi\eta a^3\Omega/T_A=15(vt/a^2)\rho/(1-\varepsilon)\rho_p$] to a smaller constant as $\lambda a\rightarrow\infty$. This outcome reflects again the behavior that a porous sphere with higher fluid permeability develops its angular velocity in percentage slower toward the terminal value. For specified values of ρ_p/ρ and λa , $(8\pi\rho a^5/T_A)d\Omega/dt$ increases with an increase in ε at the early stage (reflecting that a particle with greater porosity develops its angular velocity faster), is not a monotonic function of ε at the medium stage, and then decreases with an increase in ε at the late stage (since the particle with greater porosity has already developed most of its terminal angular velocity).

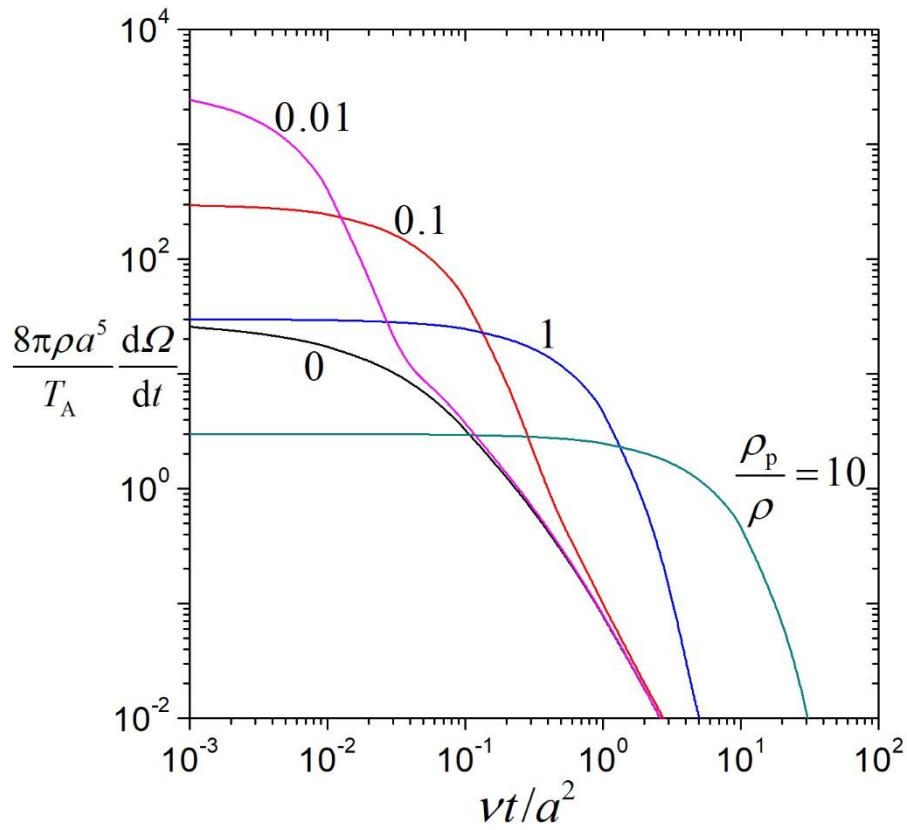
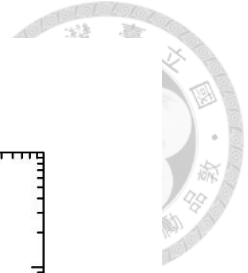


Figure A5a. Dimensionless angular acceleration $(8\pi\rho a^5/T_\Lambda)d\Omega/dt$ of a spherical porous particle in a boundless fluid versus the dimensionless elapsed time vt/a^2 with $\lambda a = 1$ and $\varepsilon = 0.5$.

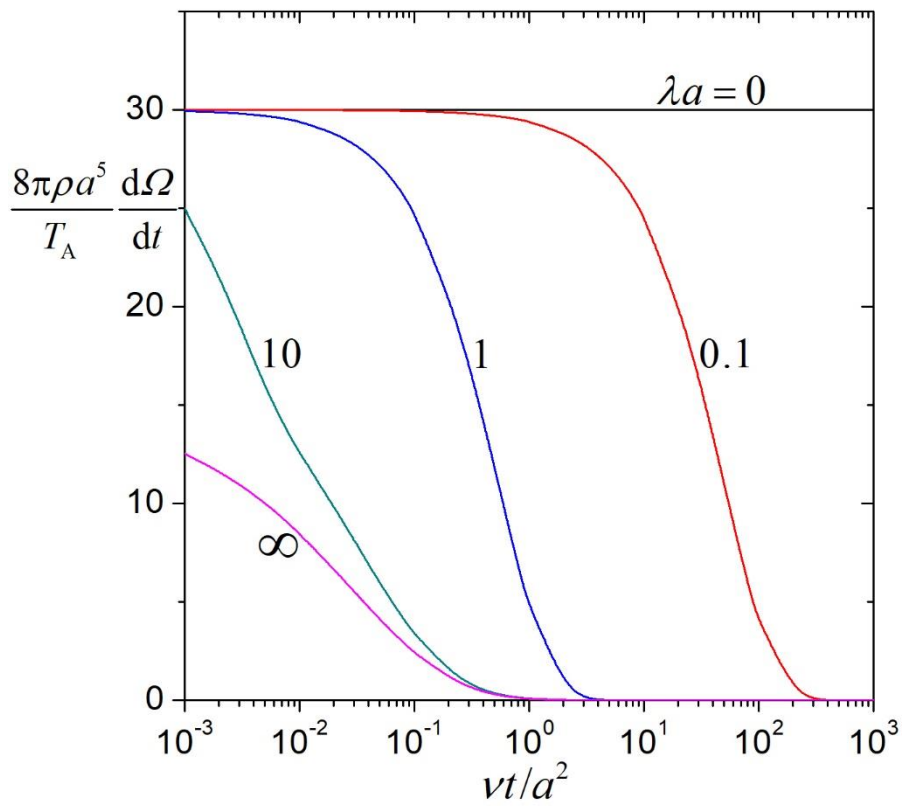
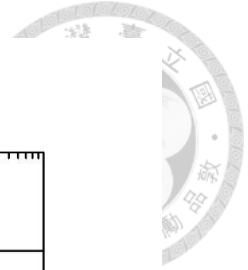


Figure A5b. Dimensionless angular acceleration $(8\pi\rho a^5/T_A)d\Omega/dt$ of a spherical porous particle in a boundless fluid versus the dimensionless elapsed time vt/a^2 with $\rho_p/\rho=1$ and $\varepsilon=0.5$.

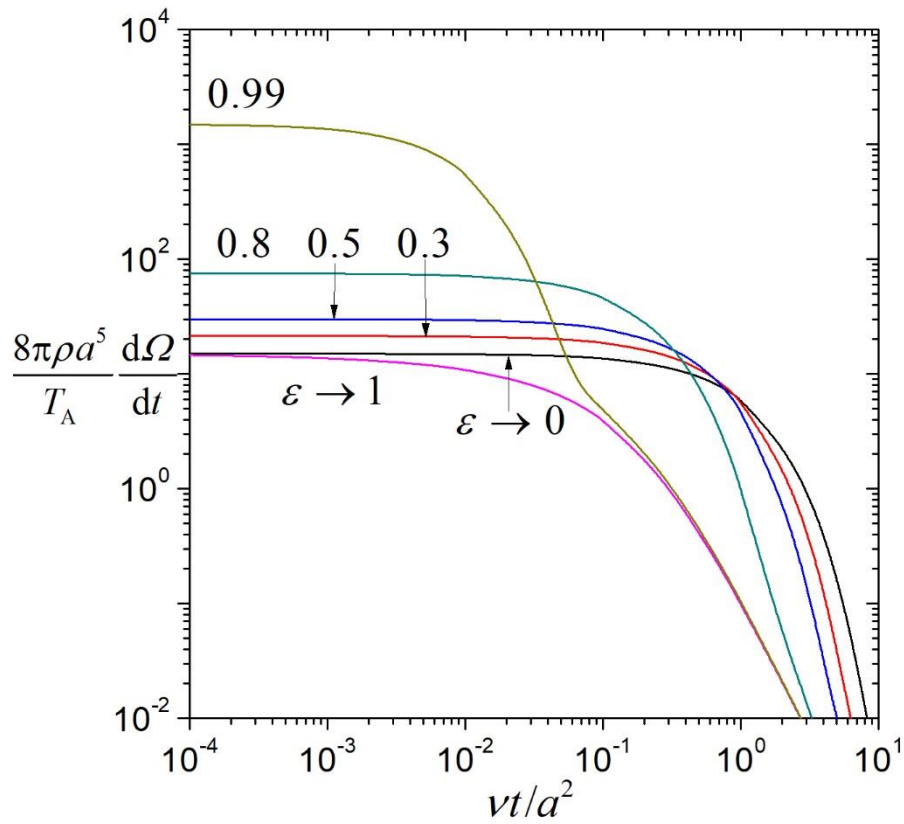
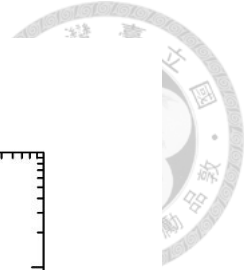
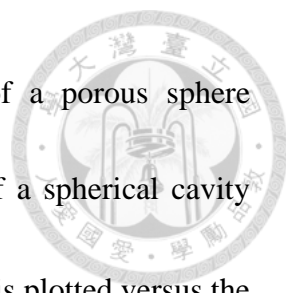


Figure A5c. Dimensionless angular acceleration $(8\pi\rho a^5/T_A)d\Omega/dt$ of a spherical porous particle in a boundless fluid versus the dimensionless elapsed time vt/a^2 with $\lambda a=1$ and $\rho_p/\rho=1$.



The dimensionless starting angular velocity $8\pi\eta a^3\Omega/T_A$ of a porous sphere applied by a constant torque T_A about a diameter at the center of a spherical cavity calculated from Eq. (A35) by means of numerical inverse transform is plotted versus the dimensionless passed time $\nu t/a^2$, ratio of the particle radius to the permeation length λa , particle-to-fluid density ratio ρ_p/ρ , and particle porosity ε in Figs. A6-A9, respectively, for several values of the particle-to-cavity radius ratio a/b . Again, $8\pi\eta a^3\Omega/T_A$ grows continuously from zero at $\nu t/a^2=0$ to the final value (which does not depend on ρ_p/ρ) given by Eq. (A3) as $\nu t/a^2 \rightarrow \infty$, diminishes monotonically with increasing λa from a constant at $\lambda a=0$ to a smaller one as $\lambda a \rightarrow \infty$, is a monotonic decreasing function of ρ_p/ρ from a constant at $\rho_p/\rho=0$ to zero as $\rho_p/\rho \rightarrow \infty$, and in general is an increasing function of ε , keeping the other parameters unchanged. For fixed values of $\nu t/a^2$, λa , ρ_p/ρ , and ε , the angular velocity $8\pi\eta a^3\Omega/T_A$ decreases monotonically with an increase in a/b (the wall retardation effect on the particle rotation is an increasing function of the relative particle radius) but in general is not a sensitive function of a/b when $\nu t/a^2$ is small (say, less than 1), λa is small (say, less than 1), ρ_p/ρ is large (say, greater than 1), or a/b is small (say, less than 0.5). For nonzero value of $\nu t/a^2$ and finite value of ρ_p/ρ , the quantity $8\pi\eta a^3\Omega/T_A$ remains finite in the limit $a/b=1$ (the cavity is filled up by the particle), except for the case of $\lambda a \rightarrow \infty$.

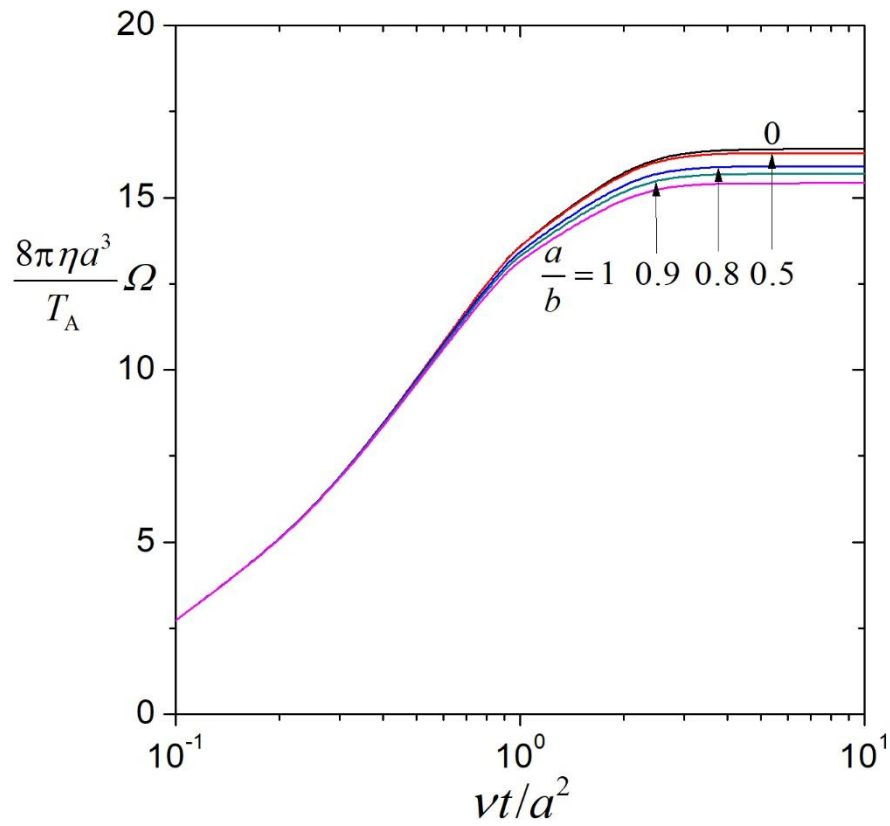


Figure A6. Dimensionless angular velocity $\frac{8\pi\eta a^3 \Omega}{T_A}$ of a spherical porous particle in a cavity versus the dimensionless elapsed time vt/a^2 with $\rho_p/\rho=1$, $\lambda a=1$, and $\varepsilon=0.5$.

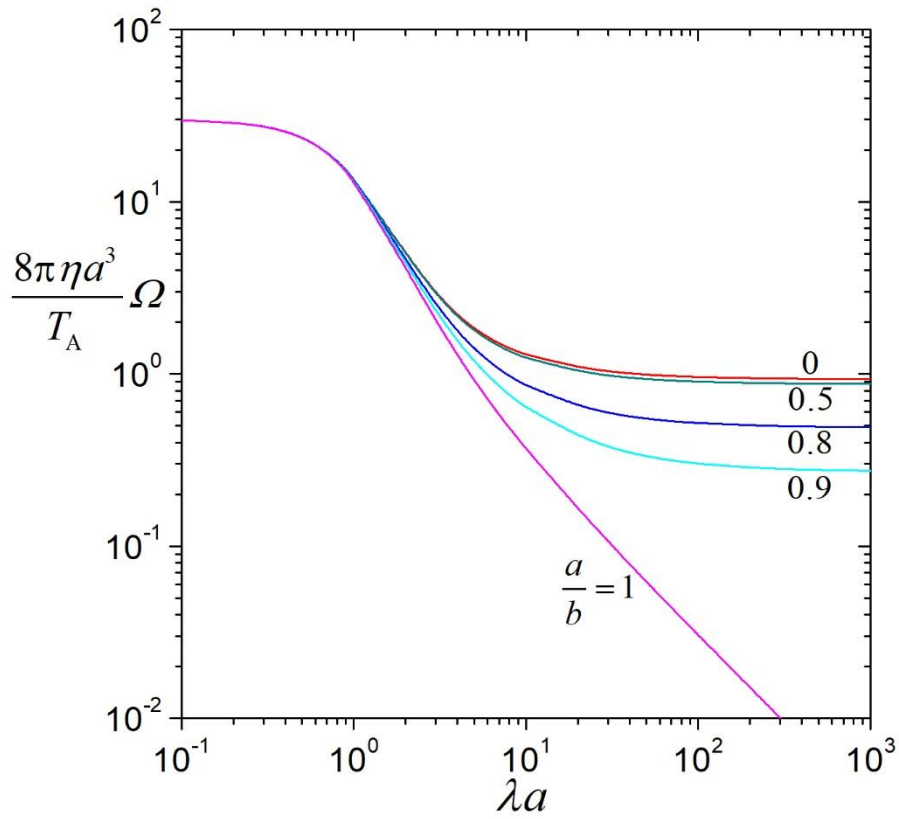


Figure A7. Dimensionless angular velocity $\frac{8\pi\eta a^3\Omega}{T_A}$ of a spherical porous particle in a cavity versus the shielding parameter λa with $vt/a^2=1$, $\rho_p/\rho=1$, and $\varepsilon=0.5$.

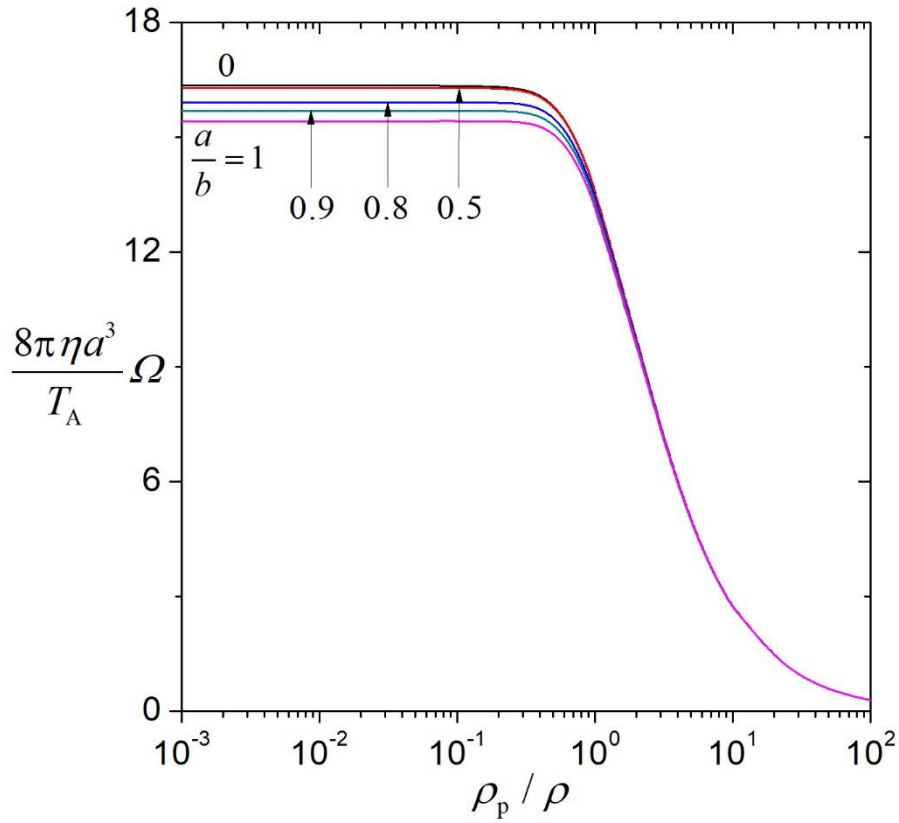


Figure A8. Dimensionless angular velocity $8\pi\eta a^3 \Omega / T_\Lambda$ of a spherical porous particle in a cavity versus the density ratio ρ_p / ρ with $vt/a^2 = 1$, $\lambda a = 1$, and $\varepsilon = 0.5$.

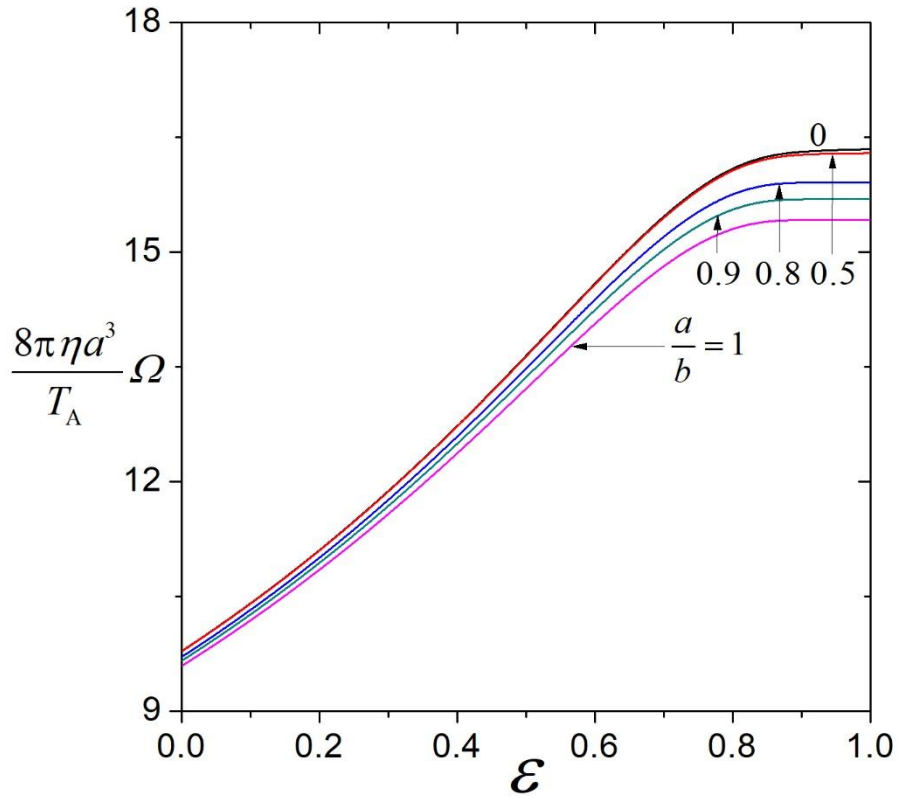
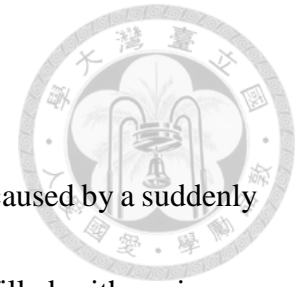


Figure A9. Dimensionless angular velocity $\frac{8\pi\eta a^3\Omega}{T_\Lambda}$ of a spherical porous particle

in a cavity versus the porosity ε with $vt/a^2=1$, $\lambda a=1$, and $\rho_p/\rho=1$.

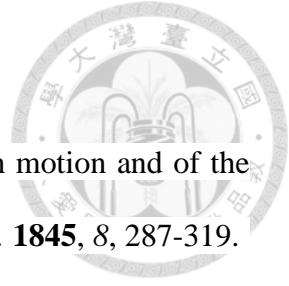
A.4 Conclusions



This appendix analyzes the start-up rotation of a porous sphere caused by a suddenly applied torque about its diameter in a concentric spherical cavity filled with a viscous fluid at low Reynolds numbers. The transient Stokes and Brinkman equations governing the fluid velocities outside and inside the porous particle, respectively, are solved by using Laplace transformation, and an explicit formula of its dynamic angular velocity as a function of the related parameters is obtained in Eq. (A35). The behavior of the starting rotation of an isolated porous particle and the effect of the confining cavity wall on the particle rotation are interesting. The angular velocity continuously increases over time from an initial zero to a terminal value and the angular acceleration continuously decays over time. A porous sphere with higher fluid permeability rotates at higher angular velocity and acceleration relative to the reference particle at any elapsed time, but lags behind it in the percentage increase in angular velocity towards the respective final values. A particle with a higher relative density or smaller porosity rotates at a lower angular velocity in any elapsed time, and the angular velocity grows slower towards the terminal value. The transient angular velocity decreases with the increase of the particle-to-cavity radius ratio, but is not a sensitive function of the radius ratio when the fluid flow resistance inside the porous particle is small, the particle-to-fluid density ratio is large, or the radius ratio itself is small. The insights gained from this theoretical research on the transient

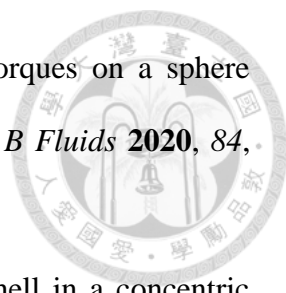
rotational motion of a porous particle at low Reynolds Numbers may hold significance in the design of micro/nanorobots [32,33].

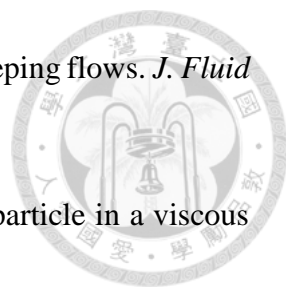




A.5 References

1. Stokes, G.G. On the theories of the internal friction of fluids in motion and of the equilibrium and motion of elastic solids. *Trans. Camb. Phil. Soc.* **1845**, 8, 287-319.
2. Stokes, G.G. On the effect of the internal friction of fluids on the motion of pendulums. *Trans. Cambridge Phil. Soc.* **1851**, 9, 8-106.
3. Brinkman, H.C. A calculation of the viscous force exerted by a flowing fluid on a dense swarm of particles. *Appl. Sci. Res.* **1947**, A1, 27-34.
4. Neale, G.; Epstein, N.; Nader, W. Creeping flow relative to permeable spheres. *Chem. Eng. Sci.* **1973**, 28, 1865-1874.
5. Matsumoto, K.; Sukanuma, A. Settling velocity of a permeable model floc. *Chem. Eng. Sci.* **1977**, 32, 445-447.
6. Masliyah, J.H.; Polikar, M. Terminal velocity of porous spheres, *Can. J. Chem. Eng.* **1980**, 58, 299-302.
7. Keh, H.J.; Chou, J. Creeping motion of a composite sphere in a concentric spherical cavity. *Chem. Eng. Sci.* **2004**, 59, 407-415.
8. Srivastava, D.K. Slow rotation of concentric spheres with source at their centre in a viscous fluid. *J. Appl. Math.* **2009**, 2009, 740172.
9. Liu, Q.; Prosperetti, A. Wall effects on a rotating sphere. *J. Fluid Mech.* **2010**, 657, 1-21.
10. Papavassiliou, D.; Alexander, G.P. Exact solutions for hydrodynamic interactions of two squirring spheres. *J. Fluid Mech.* **2017**, 813, 618-646.
11. Daddi-Moussa-Ider, A.; Lisicki, M.; Gekle, S. Slow rotation of a spherical particle inside an elastic tube. *Acta Mech.* **2018**, 229, 149-171.
12. Prakash, J. Hydrodynamic mobility of a porous spherical particle with variable permeability in a spherical cavity. *Microsystem Technol.* **2020**, 26, 2601-2614.

- 
13. Romanò, F.; des Boscqs, P.-E.; Kuhlmann, H.C. Forces and torques on a sphere moving near a dihedral corner in creeping flow. *Eur. J. Mech. B Fluids* **2020**, *84*, 110-121.
14. Keh, H.J.; Lu, Y.S. Creeping motions of a porous spherical shell in a concentric spherical cavity. *J. Fluids Struct.* **2005**, *20*, 735-747.
15. Srinivasacharya, D.; Krishna Prasad, M. Rotation of a porous approximate sphere in an approximate spherical container. *Latin Am. Appl. Res.* **2015**, *45*, 107-112.
16. Saad, E.I. Axisymmetric motion of a porous sphere through a spherical envelope subject to a stress jump condition. *Meccanica* **2016**, *51*, 799-817.
17. Sherief, H.H.; Faltas, M.S.; Saad, E.I. Stokes resistance of a porous spherical particle in a spherical cavity. *Acta Mech.* **2016**, *227*, 1075-1093.
18. Chou, C.Y.; Keh, H.J. Low-Reynolds-number rotation of a soft particle inside an eccentric cavity. *Eur. J. Mech. B Fluids* **2022**, *91*, 194-201.
19. Jhuang, L.J.; Keh, H.J. Slow axisymmetric rotation of a soft sphere in a circular cylinder. *Eur. J. Mech. B Fluids* **2022**, *95*, 205-211.
20. Chang, C.L.; Keh, H.J. Slow rotation of a soft colloidal sphere normal to two plane walls. *Colloids Interfaces* **2023**, *7*, 18.
21. Sennitskii, V.L. Unsteady rotation of a cylinder in a viscous fluid. *J. Appl. Mech. Tech. Phys.* **1980**, *21*, 347-349.
22. Buonocore, S.; Sen, M.; Semperlotti, F. A fractional-order approach for transient creeping flow of spheres. *AIP Advances* **2019**, *9*, 085323.
23. Dennis, S.C.R.; Duck, P.W. Unsteady flow due to an impulsively started rotating sphere. *Comp. Fluids* **1988**, *16*, 291-310.
24. Calabretto, S.A.W.; Levy, B.; Denier, J.P.; Mattner, T.W. The unsteady flow due to an impulsively rotated sphere. *Proc. R. Soc. A* **2015**, *471*, 20150299.

- 
25. Feng, J.; Joseph, D.D. The unsteady motion of solid bodies in creeping flows. *J. Fluid Mech.* **1995**, *303*, 83-102.
26. Ashmawy, E.A. Unsteady rotational motion of a slip spherical particle in a viscous fluid. *ISRN Math. Phys.* **2012**, *2012*, 513717.
27. Miari, N.S.; Ashmawy, E.A. Unsteady rotational motion of a composite sphere in a viscous fluid using stress jump condition. *J. Taibah Univ. Sci.* **2018**, *12*, 699-704.
28. Li, M.X.; Keh, H.J. Transient rotation of a spherical particle in a concentric cavity with slip surfaces. *Fluid Dyn. Res.* **2021**, *53*, 045509.
29. Bird, R.B.; Stewart, W.E.; Lightfoot, E.N. *Transport phenomena*, revised 2nd ed. **2007** (New York: Wiley).
30. Stehfest, H. Algorithm 368 Numerical inversion of Laplace transforms. *Comm. ACM* **1970**, *13*, 47-49.
31. Abate, J.; Valkó, P.P. Multi-precision Laplace transform inversion. *Int. J. Numer. Meth. Eng.* **2004**, *60*, 979-993.
32. Zhou, H.; Mayorga-Martinez, C.C.; Pane, S.; Zhang, L.; Pumera, M. Magnetically driven micro and nanorobots. *Chem. Rev.* **2021**, *121*, 4999–5041.
33. Yu, Z.; Li, L.; Mou, F.; Yu, S.; Zhang, D.; Yang, M.; Zhao, Q.; Ma, H.; Luo, W.; Tianlong Li, Guan, J. Swarming magnetic photonic-crystal microrobots with on-the-fly visual pH detection and self-regulated drug delivery. *InfoMat* **2023**, *5*, e12464.